

Article

Ethanollic Extract of *Polygonum minus* Protects Differentiated Human Neuroblastoma Cells (SH-SY5Y) against H₂O₂-Induced Oxidative Stress

Nor Hafiza Sayuti ^{1,2}, Nabilah Zulkefli ¹, Jen Kit Tan ², Norazalina Saad ³, Syarul Nataqain Baharum ¹, Hamizah Shahirah Hamezah ¹, Hamidun Bunawan ¹, Qamar Uddin Ahmed ⁴, Humaira Parveen ⁵, Sayeed Mukhtar ⁵, Meshari A. Alsharif ⁶ and Murni Nazira Sarian ^{1,*}

- ¹ Institute of Systems Biology (INBIOSIS), Universiti Kebangsaan Malaysia, Bangi 43600, Malaysia; norhafizasayuti@ukm.edu.my (N.H.S.); p115964@siswa.ukm.edu.my (N.Z.); nataqain@ukm.edu.my (S.N.B.); hamizahshahirah@ukm.edu.my (H.S.H.); hamidun.bunawan@ukm.edu.my (H.B.)
 - ² Department of Biochemistry, Faculty of Medicine, Universiti Kebangsaan Malaysia, Bandar Tun Razak, Cheras, Kuala Lumpur 56000, Malaysia
 - ³ UPM-MAKNA Cancer Research Laboratory, Institute of Bioscience, Universiti Putra Malaysia, Serdang 43400, Malaysia; norazalina@upm.edu.my
 - ⁴ Drug Discovery and Synthetic Chemistry Research Group, Department of Pharmaceutical Chemistry, Kulliyah of Pharmacy, International Islamic University Malaysia, Kuantan 25200, Malaysia; quahmed@iiu.edu.my
 - ⁵ Department of Chemistry, Faculty of Science, University of Tabuk, Tabuk 71491, Saudi Arabia; h.nabi@ut.edu.sa (H.P.); snoor@ut.edu.sa (S.M.)
 - ⁶ Department of Chemistry, Faculty of Applied Sciences, Umm Al-Qura University, Makkah 21955, Saudi Arabia; maasharif@uqu.edu.sa
- * Correspondence: murninazira@ukm.edu.my



Citation: Sayuti, N.H.; Zulkefli, N.; Tan, J.K.; Saad, N.; Baharum, S.N.; Hamezah, H.S.; Bunawan, H.; Ahmed, Q.U.; Parveen, H.; Mukhtar, S.; et al. Ethanollic Extract of *Polygonum minus* Protects Differentiated Human Neuroblastoma Cells (SH-SY5Y) against H₂O₂-Induced Oxidative Stress. *Molecules* **2023**, *28*, 6726. <https://doi.org/10.3390/molecules28186726>

Academic Editors: Maja Jazvinščak Jembrek and Suzana Šegota

Received: 21 August 2023

Revised: 13 September 2023

Accepted: 18 September 2023

Published: 20 September 2023



Copyright: © 2023 by the authors. Licensee MDPI, Basel, Switzerland. This article is an open access article distributed under the terms and conditions of the Creative Commons Attribution (CC BY) license (<https://creativecommons.org/licenses/by/4.0/>).

Abstract: Neuronal models are an important tool in neuroscientific research. Hydrogen peroxide (H₂O₂), a major risk factor of neuronal oxidative stress, initiates a cascade of neuronal cell death. *Polygonum minus* Huds, known as ‘kesum’, is widely used in traditional medicine. *P. minus* has been reported to exhibit a few medicinal and pharmacological properties. The current study aimed to investigate the neuroprotective effects of *P. minus* ethanollic extract (PMEE) on H₂O₂-induced neurotoxicity in SH-SY5Y cells. LC-MS/MS revealed the presence of 28 metabolites in PMEE. Our study showed that the PMEE provided neuroprotection against H₂O₂-induced oxidative stress by activating the Nrf2/ARE, NF-κB/IKB and MAPK signaling pathways in PMEE pre-treated differentiated SH-SY5Y cells. Meanwhile, the acetylcholine (ACH) level was increased in the oxidative stress-induced treatment group after 4 h of exposure with H₂O₂. Molecular docking results with acetylcholinesterase (AChE) depicted that quercitrin showed the highest docking score at −9.5 kcal/mol followed by aloe-emodin, afzelin, and citreosein at −9.4, −9.3 and −9.0 kcal/mol, respectively, compared to the other PMEE’s identified compounds, which show lower docking scores. The results indicate that PMEE has neuroprotective effects on SH-SY5Y neuroblastoma cells in vitro. In conclusion, PMEE may aid in reducing oxidative stress as a preventative therapy for neurodegenerative diseases.

Keywords: *Polygonum minus*; oxidative stress; antioxidant; neuron; neuroprotective; hydrogen peroxide; acetylcholine; molecular docking; LC-MS/MS

1. Introduction

Oxidative stress is a condition that happens when there is an imbalance between oxidants and antioxidants in a living system. It is linked to many neurological disorders including Alzheimer’s disease, Huntington’s disease, Parkinson’s disease, and amyotrophic lateral sclerosis. The imbalance happens when there are too many reactive oxygen species (ROS) or when the antioxidant system does not work appropriately [1]. The body has specific defense mechanisms in the form of endogenous antioxidants, such as glutathione,

and antioxidant enzymes, such as superoxide dismutase (SOD), glutathione peroxidase (GPX), and catalase, which combat the harmful effects of excessive ROS [2]. A growing body of research has revealed that, under normal conditions, oxidative damage causes reactions that have a negative impact on beneficial markers in the antioxidant mechanistic pathway that is responsible for neutralizing harmful stimuli. Exogenous antioxidants, on the other hand, tend to counteract such effects, but when present in large quantities, they inhibit the response generated by their indigenous counterpart, increasing the cells' sensitivity to stimuli and eventually leading to death [3–5]. The antioxidant properties of plant materials for maintaining health and preventing various diseases prompted scientists to investigate various herbs.

Polygonum minus Huds is a well-known traditional herbal plant in Malaysia, and it is commonly referred to as 'kesum' in the Malay language [6]. Various *Polygonum* species have demonstrated antioxidant properties [7,8]. *P. minus* is a plant with a high concentration of flavonoids and other antioxidants that reduce oxidative stress in neuronal membranes [9]. *P. minus* has been shown to have in vitro antioxidant properties, low-density lipoprotein (LDL) oxidation inhibition, antiulcer activity, analgesic activity, anti-inflammatory activity, antiplatelet aggregation activity, antimicrobial activity, digestive enhancing property, and cytotoxic activity [10–15]. Researchers have linked this plant's pharmacological effects to its high antioxidant capacity. This plant's aqueous, methanolic, and ethanolic extracts demonstrated high antioxidant activity, which was primarily attributed to its phenolic compounds [10,16–18]. The isolated compounds from *P. minus* such as polygonumins A [19], polygonumins B, C, and D [6] were reported to have diverse potential medicinal activities. In a study conducted by Yaacob [20], it was found that decanal and dodecanal are the primary aldehydes responsible for contributing flavor to *P. minus*. In addition to decanal and dodecanal, Yaacob's analysis revealed the presence of several other compounds in *P. minus*, including 1-decanol, 1-dodecanol, undecanal, tetradecanal, 1-undecanol, nonanal, 1-nonanol, and β -caryophyllene. In a study carried out by Baharum et al. [21], a total of 42 compounds were successfully identified using gas chromatography–mass spectrometry (GC–MS). This number greatly exceeded the count given by Yaacob [20]. Some of the compounds found included α -pinene, drimenol, humulene, caryophyllene, farnesol, neoisolongifolene, 8-bromo-, and isobornyl acetate. To date, the literature on the neuroprotective effect of *P. minus* is still lacking. Thus, this present study aims to determine whether *P. minus* ethanolic extract (PMEE) can protect differentiated human neuroblastoma SH-SY5Y cells from H₂O₂-mediated oxidative stress.

2. Results and Discussion

2.1. LC–MS/MS Analysis

The positive and negative LC–MS/MS chromatograms of PMEE were shown in Figure 1. The presence of peaks in the chromatogram indicated the presence of various PMEE-derived compounds. The LC–MS/MS characterization of the phenolic compounds in PMEE revealed the presence of 28 metabolites, listed in Table 1. These metabolites have a variety of therapeutic properties, including anti-inflammatory, antioxidant, and anticancer properties.

In Table 1, PMEE was shown to contain various classes of natural compounds such as caffeic acid, (–)-epicatechin, kaempferol, gallic acid, eupatilin (5,7-dihydroxy-3',4',6-trimethoxyflavone) and rhamnetin (7-methylquercetin) which have been proven to play a role in scavenging H₂O₂ and preventing cell damage by oxidative stress [22–27]. On the other hand, quercetin and quercitrin reduced the accumulation of ROS and nitric oxide while protecting against cytokine-induced cell death [28]. Meanwhile, Kwon et al. [29] demonstrated the neuroprotective activity of quinic acid isolated from the roots of *Arctium lappa* Linne. It protected PC12 cells from oxidative stress, which could be attributed to the antioxidant capacity of quinic acid [29]. The detection of various phenolic compounds, based on compound identification, strengthens the suggestion that other bioactive com-

pounds in addition to polyphenols or flavonoids were also present and contributed to the diverse bioactive characteristics of *P. minus*.

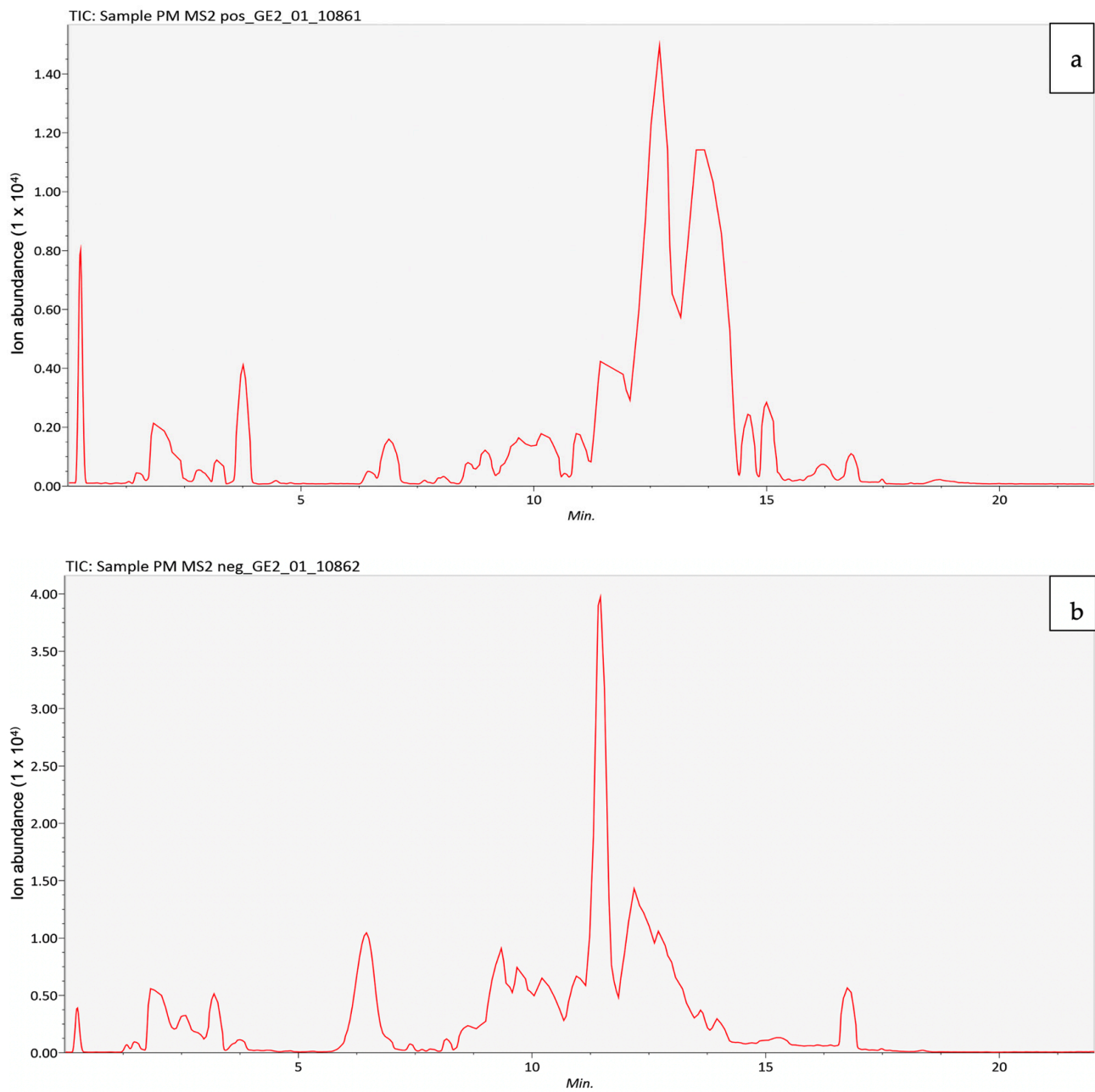


Figure 1. Liquid chromatography–mass spectrophotometry (LC–MS/MS) analysis of PMEE in the positive mode (a) and the negative mode (b).

Table 1. List of compounds identified in PMEE by LC–MS/MS analysis.

No	Identified Compounds	Retention Time (min)	Molecular Formula	Molecular Weight (g/mol)
1	Quinic acid	2.540	C ₇ H ₁₂ O ₆	191.06
2	Gallic acid	6.456	C ₇ H ₆ O ₅	169.01
3	2,3-Dihydroxybenzoic acid	8.170	C ₇ H ₆ O ₄	153.02
4	(–)-epicatechin	8.686	C ₁₅ H ₁₄ O ₆	291.09
5	5-Hydroxy-2-penten-1-yl-3-oxocyclopentyl acetic acid	8.753	C ₁₂ H ₁₈ O ₄	227.13
6	Caffeic acids	9.142	C ₉ H ₈ O ₄	179.04
7	Loliolide	9.506	C ₁₁ H ₁₆ O ₃	197.12
8	Quercitrin	9.673	C ₂₁ H ₂₀ O ₁₁	449.11
9	Naphtho[2,3-b]furan-9(4H)-1,4,8-bis(acetyloxy)-4a,5,6,7,8,8a-hexahydro-3,4a,5-trimethyl-, (4S,4aR,5S,8S,8aS)	9.823	C ₁₉ H ₂₄ O ₆	331.15
10	Carboxymethyl-cyclohexanecarboxylic acid	9.961	C ₉ H ₁₄ O ₄	185.08
11	Afzelin	10.073	C ₂₁ H ₂₀ O ₁₀	433.11
12	6-Hydroxy-3-isopropylidene-4a,5-dimethyl-4,4a,5,6,7,8-hexahydro-2(3H)-naphthalenone	10.157	C ₁₅ H ₂₂ O ₂	235.17
13	Feruloyltyramine	10.157	C ₁₈ H ₁₉ NO ₄	314.14
14	Daphnetin	10.362	C ₉ H ₆ O ₄	177.02
15	Esculetin	10.423	C ₉ H ₆ O ₄	179.03
16	Citreorosein	10.910	C ₁₅ H ₁₀ O ₆	287.05
17	Quercetin	11.428	C ₁₅ H ₁₀ O ₇	303.05
18	Aloe-emodin	12.250	C ₁₅ H ₁₀ O ₅	271.06
19	Kaempferol	12.250	C ₁₅ H ₁₀ O ₆	287.05
20	Rhamnetin	12.250	C ₁₆ H ₁₂ O ₇	317.06
21	(2Z)-4,6-dihydroxy-2-[(4-hydroxy-3,5-dimethoxyphenyl)methylidene]-1-benzofuran-3-yl	12.516	C ₁₇ H ₁₄ O ₇	331.08
22	Eupatilin	12.516	C ₁₈ H ₁₆ O ₇	345.09
23	Corynoxine	12.971	C ₂₂ H ₂₆ N ₂ O ₄	383.20
24	Valerenic acid	13.062	C ₁₅ H ₂₂ O ₂	233.16
25	alpha-Cyperone	13.154	C ₁₅ H ₂₂ O	219.17
26	Dibutylphthalate	13.304	C ₁₆ H ₂₂ O ₄	279.16
27	(2Z)-2-[(E)-6-(hydroxymethyl)-2,4,8,10-tetramethyldodec-2-enylidene]-4-methylpentanedioic acid	13.847	C ₂₃ H ₄₀ O ₅	419.27
28	Prespatane	14.260	C ₁₅ H ₂₄	205.19

2.2. Phase Contrast Microscopy and Immunocytochemistry Confirmed Neuronal Marker β -Tubulin III Expression

To demonstrate the neuronal phenotype of differentiated SH-SY5Y used in this study, the cells were examined under a fluorescence microscope using the phase contrast mode. Figure 2a shows that undifferentiated cells had no or significantly fewer neurites. In contrast, after seven days of differentiation, the neurite characteristics persisted and grew in the differentiated cells (Figure 2b), indicating that the SH-SY5Y cells had differentiated into typical neuronal cells. Immunocytochemistry was performed on differentiated cells in addition to morphological evaluation of SH-SY5Y-derived neuronal cells to evaluate the differentiation process. Undifferentiated and differentiated SH-SY5Y cells were stained and incubated with antibodies against the neuron-specific protein β -tubulin III, which is a marker of neurite development. The undifferentiated but stained cells showed low green fluorescence in the cytoplasm or neurite (Figure 2c), indicating that the marker was not present within the cells. Figure 2b,d show the morphological changes observed in the SH-SY5Y cell population throughout the differentiation period. Greenish fluorescence was observed in differentiated cells' cytoplasm and neurites (Figure 2d), indicating a

high level of β -tubulin III expression in both the cytoplasm and neurites of differentiated SH-SY5Y cells. Similar findings have been reported in previous studies [30,31], in which RA treatment resulted in neurite extension in SH-SY5Y cells. Phase contrast microscopy confirmed the success of the differentiation process. Consequently, differentiated cells were used throughout the experiment.

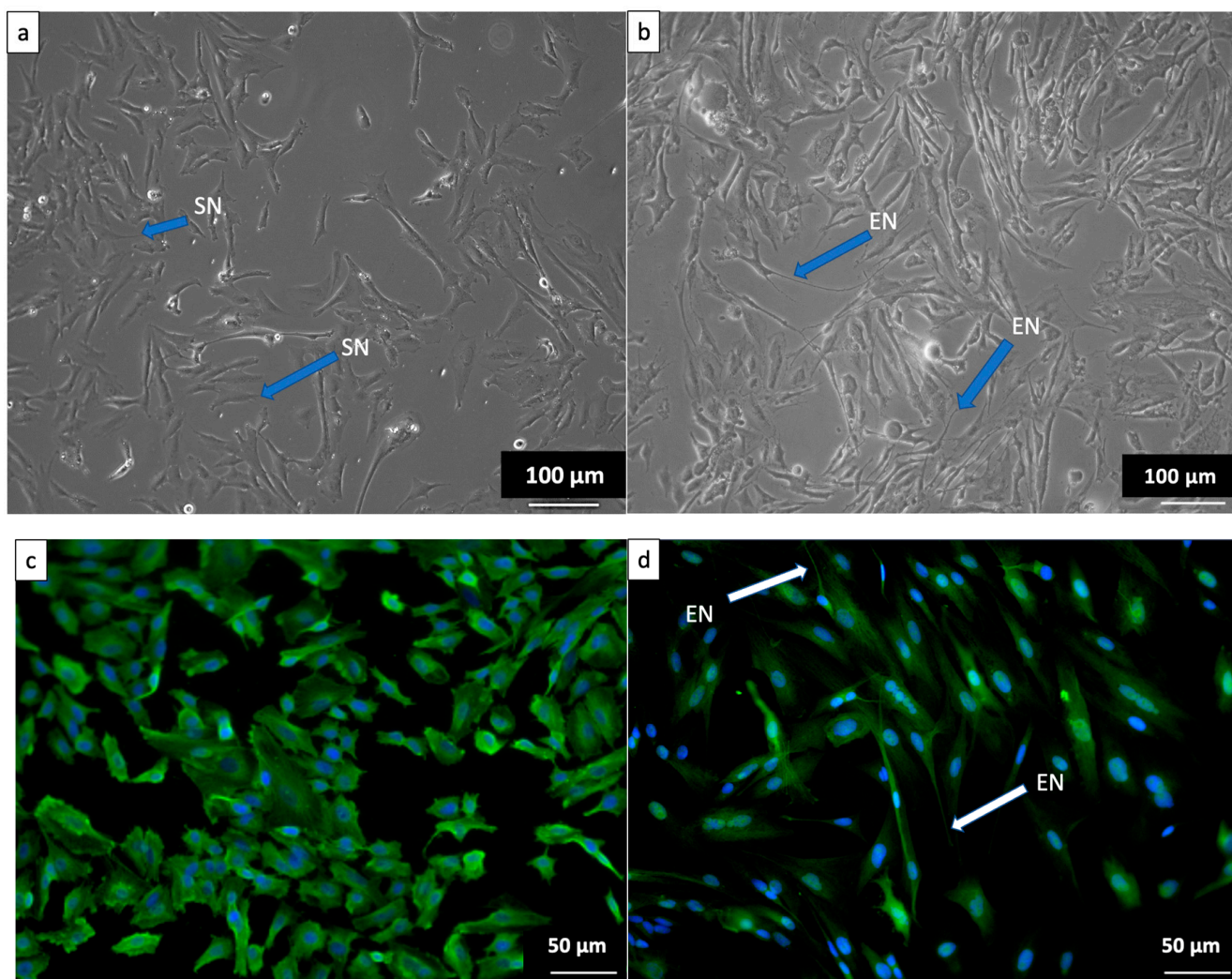


Figure 2. The image shows SH-SY5Y cells observed in phase contrast microscopy (**upper**) and differentiated SH-SY5Y cells observed in fluorescence microscopy (**lower**). (a) Undifferentiated SH-SY5Y cells cultured in complete growth media, (b) differentiated SHSY-5Y cells cultured in complete differentiation media treated with 10 μ M retinoic acid (RA) for 7 days, (c) fluorescence micrograph of undifferentiated cells and the image (d) showing the extension of SH-SY5Y neurites after 7-day differentiation with 10 μ M RA. SN: short neurites. EN: extended neurites. Magnification ((a,b): 10 \times ; (c,d): 20 \times).

2.3. Cytotoxicity Effect of PMEE and H_2O_2 on SH-SY5Y Viability

The MTT assay was used to determine cell viability in differentiated SH-SY5Y cells. The cells were exposed to PMEE at various concentrations (0.5 to 1000 μ g/mL) for 24, 48, and 72 h. As shown in Figure 3, the PMEE-treated cells were viable across the concentrations used in a time-dependent manner. A similar pattern was observed in cells treated with curcumin at various concentrations (0.8 to 100 μ g/mL) for 24, 48, and 72 h (Figure 4). As described in Section 3.6, the cytotoxicity of H_2O_2 was also determined by exposing differentiated cells to H_2O_2 at various concentrations (7.8 to 1000 μ M/mL) for 4 h. In

4 h, 220 μM H_2O_2 caused approximately 50% cell death, according to the results obtained. Therefore, it was selected as the concentration of H_2O_2 to challenge PMEE pre-treated cells in the subsequent experiments. According to studies, exposing differentiated SH-SY5Y cells to cytotoxic agents such as hydrogen peroxide for a predetermined period results in oxidative stress and cell death. Several prior studies have demonstrated that H_2O_2 has a cytotoxic effect on differentiated SH-SY5Y cells used as a model for neuroprotection research [31,32]. Furthermore, it was observed that the use of *P. minus* extract at doses of up to 500 $\mu\text{g}/\text{mL}$ did not exhibit any harmful effects on normal human lung fibroblast cell line (Hs888Lu) [33]. Ghazali et al. [34] studied the antiproliferative effect of various solvent extracts of *P. minus* using in vitro MTT assay against HepG2, WRL68, HeLa, HCT 116, MCF-7 and Chang cell lines. The ethanol extract showed lowest IC_{50} of 32.25 ± 3.72 $\mu\text{g}/\text{mL}$ towards HepG2 cell lines with minimum toxicity in WRL68 normal embryonic liver cells whereas methanol extract showed moderate antiproliferative activity against HCT 116 cell lines ($\text{IC}_{50} = 56.23 \pm 3.2$ $\mu\text{g}/\text{mL}$) [34]. *P. minus* had cytotoxic effects on cancer cells while demonstrating minimal toxicity towards normal cells. This shows that *P. minus* exhibits a selective effect in safeguarding normal cells.

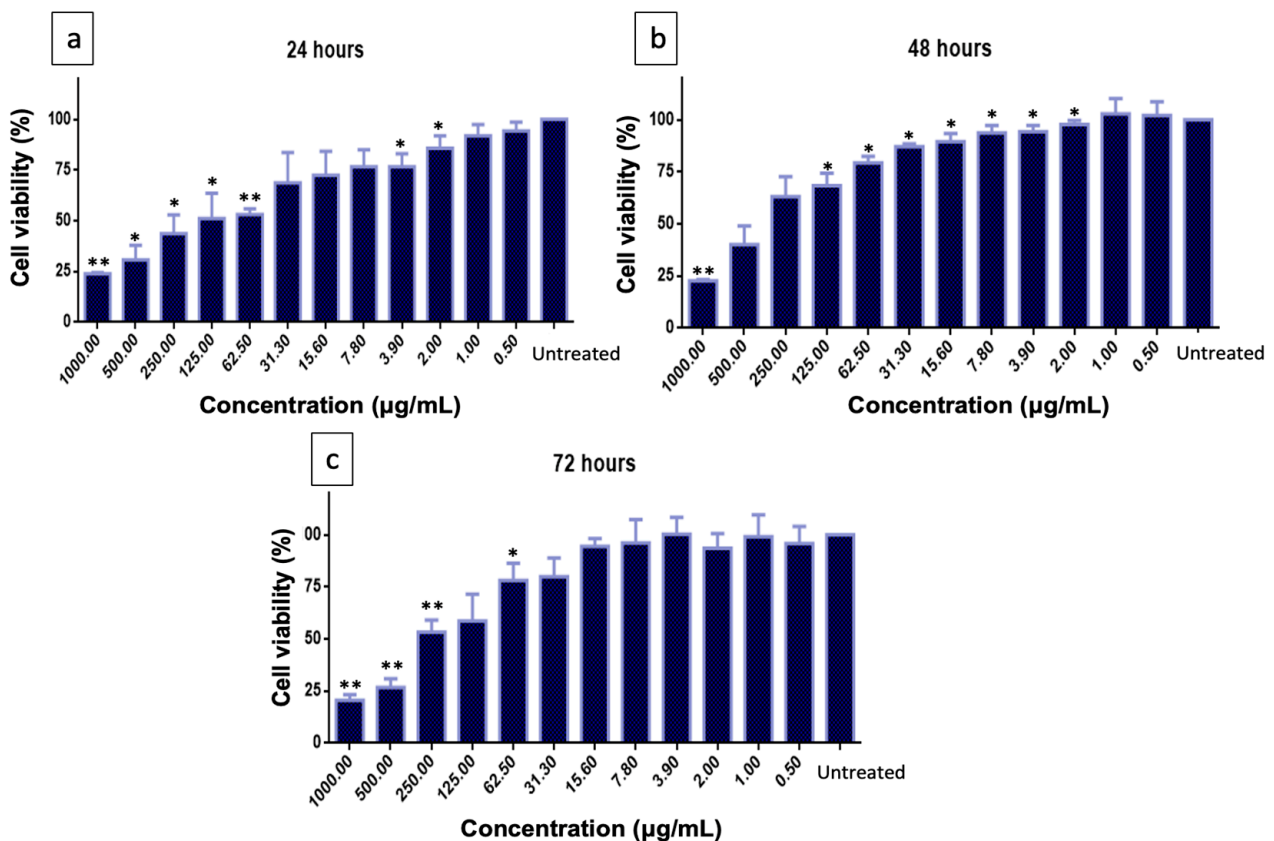


Figure 3. Cytotoxicity of PMEE on differentiated SH-SY5Y cells. (a) Viable cells after 24 h, (b) after 48 h, and (c) after 72 h. The values are the means of three independent trials ($n = 3$) and means with asterisks differed significantly ($* p < 0.05$, $** p < 0.01$) with the untreated control.

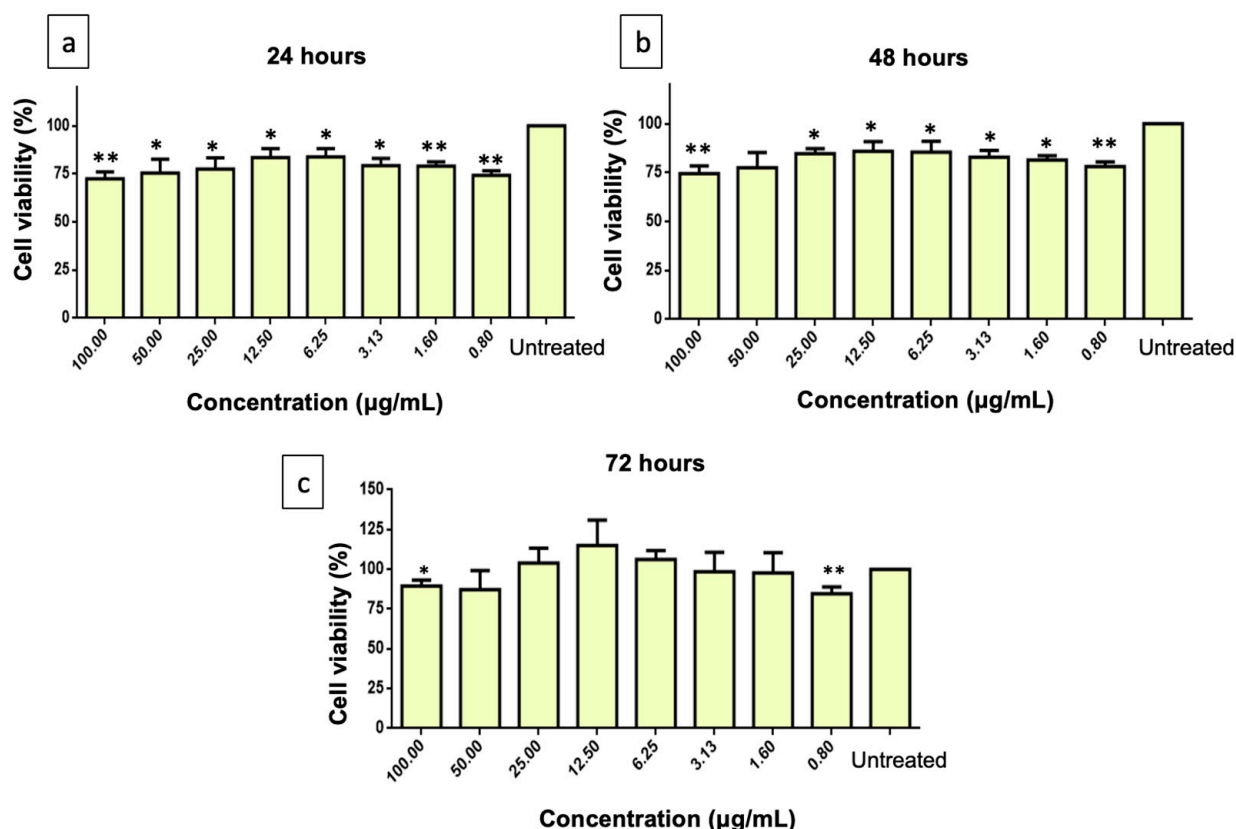


Figure 4. Cytotoxicity of curcumin on differentiated SH-SY5Y cells. (a) Cell viability after 24 h, (b) 48 h and (c) 72 h. The values are the means of three independent trials ($n = 3$) and means with asterisks differed significantly (* $p < 0.05$, ** $p < 0.01$) with the untreated control.

2.4. Neuroprotective Effect of PMEE against H_2O_2 -Induced Cytotoxicity

Damage to neurons resulting from oxidative stress (primarily reactive oxygen species) is one of the leading causes of neurodegenerative diseases [35]. To evaluate the neuroprotective effect of PMEE and curcumin against H_2O_2 -induced cell death, the differentiated SH-SY5Y cells were pre-treated with a range of PMEE (0.5 to 1000 $\mu\text{g/mL}$) and curcumin (0.8 to 100 $\mu\text{g/mL}$) for 24, 48, and 72 h. Then, the pre-treated cells were exposed to IC_{50} of H_2O_2 (220 μM) for 4 h. MTT assay showed that H_2O_2 inhibited the cells' viability, while pre-treatment of the cells with PMEE provided protection to the cells against the cytotoxic effect of H_2O_2 across the experimental period (Figure 5a–c) when compared to untreated control cells. However, pre-treatment with 62.5 $\mu\text{g/mL}$ of PMEE demonstrated the highest viability against H_2O_2 especially after 48 and 72 h (Figure 5d). Moreover, 3.13 $\mu\text{g/mL}$ of curcumin demonstrated the highest viability effect on the differentiated cells after 48 h of pre-treatment (Figure 5e). Hence, they were selected as working concentrations for the rest and standard control in the subsequent experiments.

The potential utilization of herbal medicines as a novel preventative neuroprotective strategy in the context of neurodegenerative illnesses is a subject of interest. These natural therapies could be explored for their applicability in individuals who are at risk of developing such conditions [36]. Exogenous antioxidants have been shown in studies to help prevent oxidative damage by reducing ROS production in cells, increasing their chances of survival [3,5]. The current findings demonstrated how different concentrations of PMEE increased the viability of differentiated neurons in a time and dose-dependent manner. However, 62.5 $\mu\text{g/mL}$ of PMEE demonstrated the greatest potential in that regard, indicating a high capability for reducing susceptibility caused by hermetic response in the cells. The effect was clearly greater after 48 and 72 h of treatment than after 24 h. This is due to the long-term effect on endogenous defensive mechanisms, which reduces the cells'

vulnerability to attack from endogenous cytotoxic agents. Previous research found that an ethyl acetate extract of *P. minus* has a selective antiproliferative effect on HepG2 cells while having little cytotoxicity on normal liver cells [34].

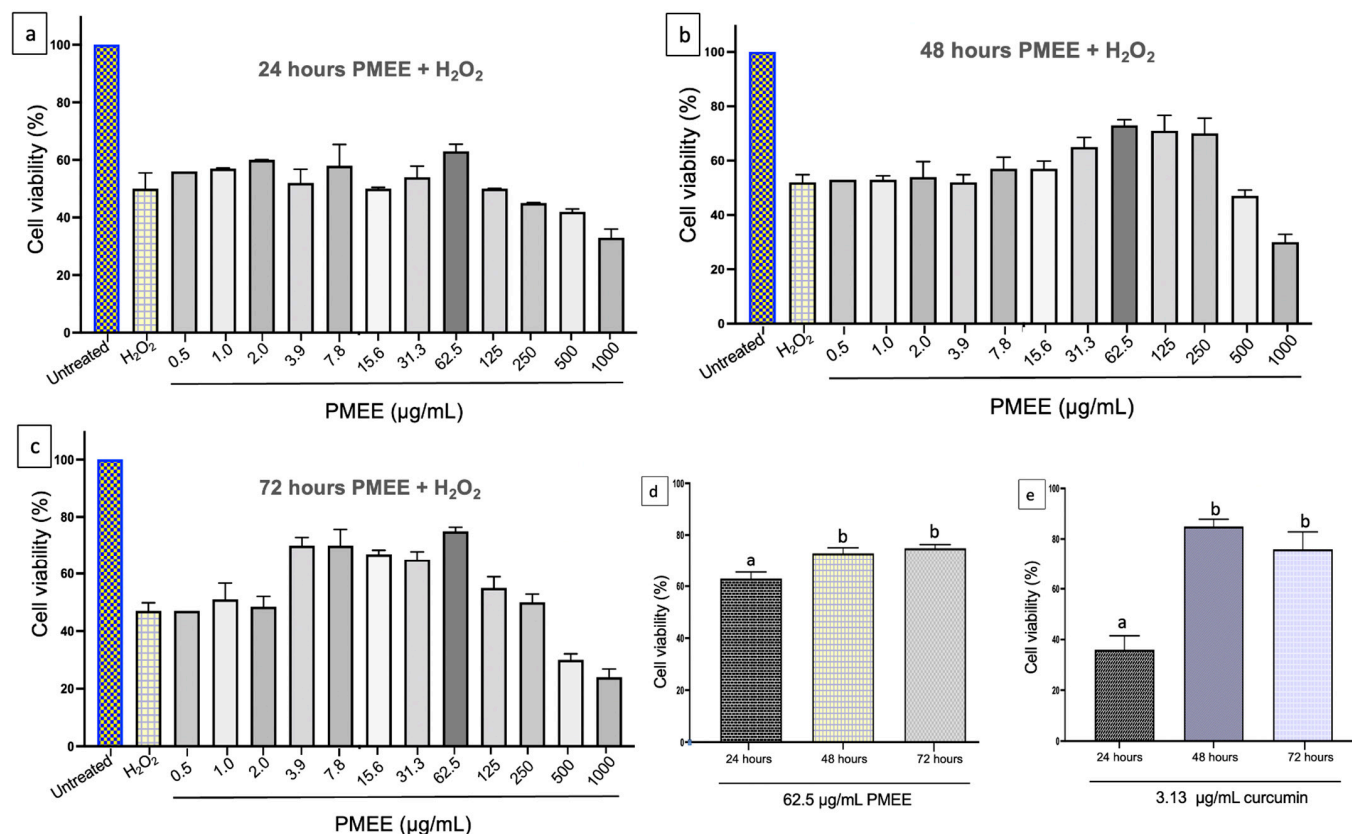


Figure 5. PMEE has a concentration-dependent neuroprotective effect. The differentiated SH-SY5Y cells were pre-treated with PMEE (0.5–1000 g/mL) for (a) 24, (b) 48, and (c) 72 h before being exposed to 220 µM H₂O₂ for 4 h. (d) A total of 62.5 µg/mL of PMEE and (e) 3.13 µg/mL of curcumin plus 4 h of exposure to 220 µM of H₂O₂. The values are the means of three independent trials (n = 3) and the means with different alphabets vary significantly ($p < 0.05$).

2.5. PMEE Pre-Treatment Influenced Gene Expressions in Nrf2/ARE Pathway

The expression level of Nrf2, NQO1, SOD1, SOD2, and catalase under the Nrf2/ARE signaling pathway increased significantly ($p < 0.05$) in cells exposed to PMEE plus 4 h of H₂O₂ compared to cells treated with PMEE alone (Figure 6). The pre-treatment of differentiated neuron cells with PMEE increased the expression of these genes above the normal level. When Nrf2 is released from the cytoplasm, it translocates to the nucleus as a transcription factor. The factor binds to the antioxidant response element (ARE) to form a complex that binds to the promoter region of phase II antioxidant genes to initiate transcription of the phase II antioxidant proteins, which play a role in counteracting the toxic effects of free radicals and protecting neurons from damage and death [37]. Though under oxidative stress, the presence of PMEE enhanced the expression of Nrf2 genes and their translocation to the nucleus. In addition, the increased expression of NQO1 in cells pre-treated with PMEE suggests a potential gene-level neuroprotective effect of PMEE.

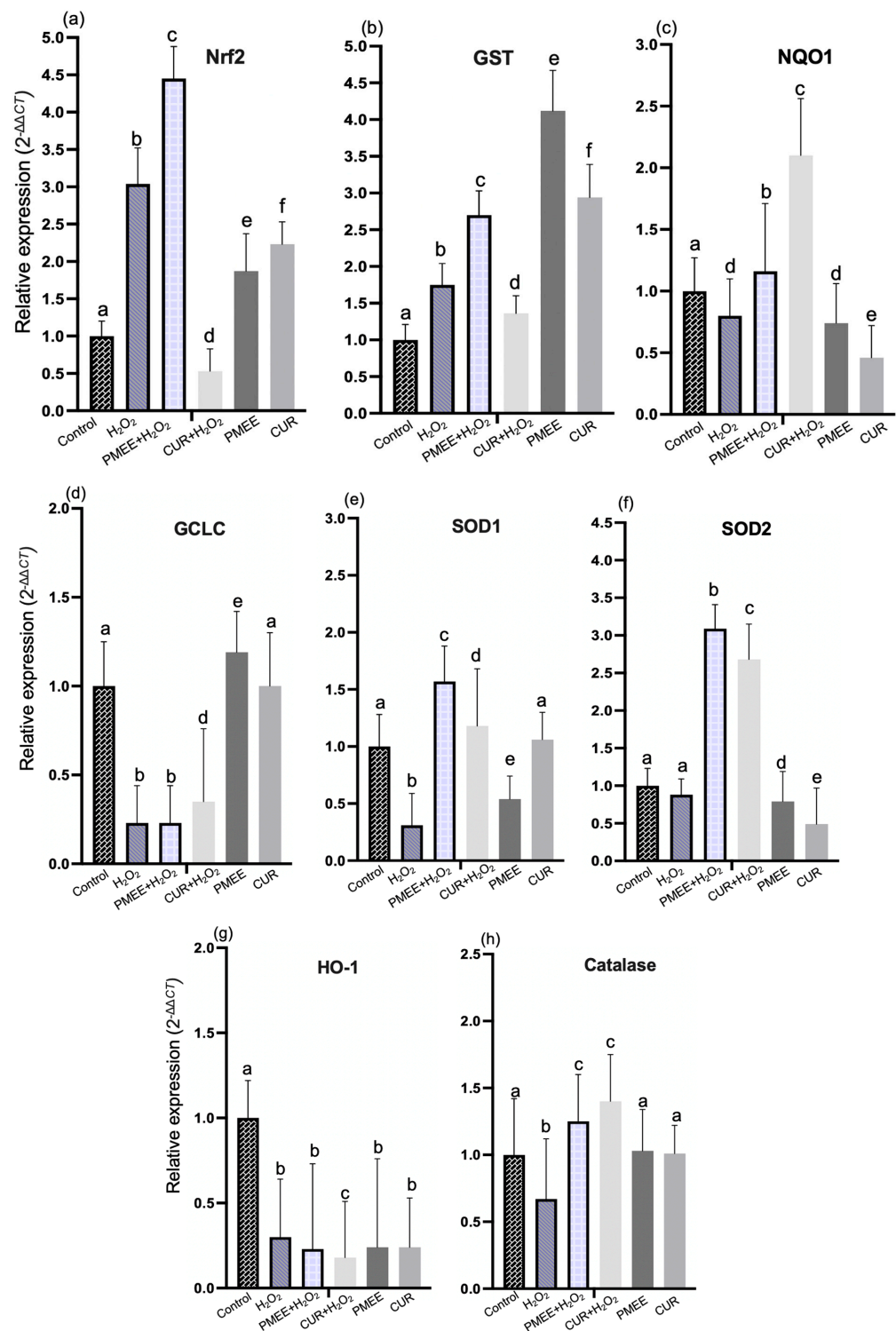


Figure 6. The mRNA expression of (a) Nrf2, (b) GST, (c) NQO1, (d) GCLC, (e) SOD1, (f) SOD2, (g) HO-1 and (h) catalase in the Nrf2/ARE signaling pathway. Control: untreated cells; H₂O₂: cells induced with 300 μM hydrogen peroxide for 4 h; PMEE + H₂O₂: cells pre-treated with PMEE for 48 h + 4 h exposure to H₂O₂; CUR+H₂O₂: cells pre-treated with curcumin for 48 h + 4 h exposure to H₂O₂; PMEE: cells treated with only PMEE; CUR: cells treated with only curcumin. The value represents fold changes between control (untreated cells) and treatment groups. Data were expressed as the mean ± SD of triplicate experiments; values with different letters alphabets are significantly different from one another and vice versa ($p < 0.05$).

The mRNA level of the GST gene increases significantly ($p < 0.05$) when the cells are pre-treated with PMEE with or without an H_2O_2 challenge compared to the H_2O_2 control group (Figure 6b). GST proteins are significant antioxidant enzymes that regulate stress-induced signaling pathways and are essential for scavenging the free radicals produced by cells [38]. Increased expression or activity of this enzyme indicated improved antioxidant activity. PMEE's ability to prevent neuronal death caused by oxidative stress was indicated by its ability to increase GST expression. PMEE pre-treatment prior to H_2O_2 exposure resulted in a significant ($p < 0.05$) decrease in the mRNA expression level of the GCLC gene in differentiated SH-SY5Y cells compared to PMEE alone (Figure 6d). The GCLC encodes glutamate-cysteine ligase, a phase II antioxidant marker with extraordinary antioxidant activity in humans and other closely related species [31]. In reaction to oxidative stress as well as other inflammatory factors, the level of GCLC increases to neutralize the harmful environmental effect and ensure the survival of affected cells. However, inducing H_2O_2 for 4 h in PMEE pre-treatment differentiated SH-SY5Y cells did not enhance the expression level of GCLC.

SOD1 and SOD2 gene expression increased significantly ($p < 0.05$) in differentiated cells treated with PMEE prior to H_2O_2 exposure, as compared to control cells and cells treated with PMEE alone (Figure 6e,f). The two genes code for the enzyme's superoxide dismutase 1 and 2, which are abundant in neural tissue. Part of the physiological and antioxidant significance of these proteins is their ability to regulate superoxide concentration by converting superoxide to hydrogen peroxide, a substrate for another phase II enzyme that is less damaging to the former [39]. This phenomenon facilitates neuron cell survival in a toxic environment. In contrast, the expression of the HO-1 gene decreased significantly ($p < 0.05$) in all treatment groups (Figure 6g) compared to untreated cells. This indicates that treatment exposure had no effect on the expression of HO-1 in differentiated SH-SY5Y cells. Moreover, after 48 h, the level of mRNA for catalase gene expression increased significantly ($p < 0.05$) in PMEE pre-treated cells plus 4 h of H_2O_2 exposure compared to its expression in H_2O_2 control and PMEE-treated cells (Figure 6h). Catalase plays a crucial antioxidant role in the body by converting harmful substances, such as cellular hydrogen peroxide, into less toxic forms (oxygen or water) [40].

2.6. PMEE Pre-Treatment Influenced Gene Expressions in NF- κ B/I κ B Pathway

In oxidative stress conditions with or without PMEE and curcumin, the mRNA expression level of genes involved in the NF- κ B/I κ B-mediated neuropathological pathway is drastically altered. This pathway is influenced by NF- κ B, I κ B, BACE1, APP, and MAPT genes. All gene expression levels were significantly ($p < 0.05$) higher in PMEE-treated cells than in H_2O_2 control cells (Figure 7). Pre-treatment of differentiated SH-SY5Y cells with PMEE for 72 h inhibited the overexpression of the NF- κ B gene significantly ($p < 0.05$) when the cells were exposed to an H_2O_2 -induced toxic environment for 4 h, as compared to its high expression in the PMEE-only treatment group (Figure 7a). Reportedly, inhibition of NF- κ B mediates neuroprotection in neurodegenerative diseases such as Alzheimer's and multiple sclerosis [41]. The present findings suggested that PMEE could selectively inhibit the expression of NF- κ B subunits, which are accountable for the transcription of inflammatory markers that induce neuronal damage and death. PMEE pre-treatment prior to H_2O_2 exposure significantly ($p < 0.05$) increased the level of mRNA for the I κ B gene in differentiated neuron cells compared to H_2O_2 control cells (Figure 7b). The I κ B gene encodes the I κ B α protein, which prevents the production of inflammatory cytokines. I κ B α and NF- κ B interact in two ways: by retaining the transcription factor (NF- κ B) in the cytoplasm and by inhibiting its DNA binding in the nucleus. PMEE perhaps strengthened the interaction between the two molecules by preventing phosphorylation of I κ B α which leads to the release of NF- κ B and its translocation to the nucleus.

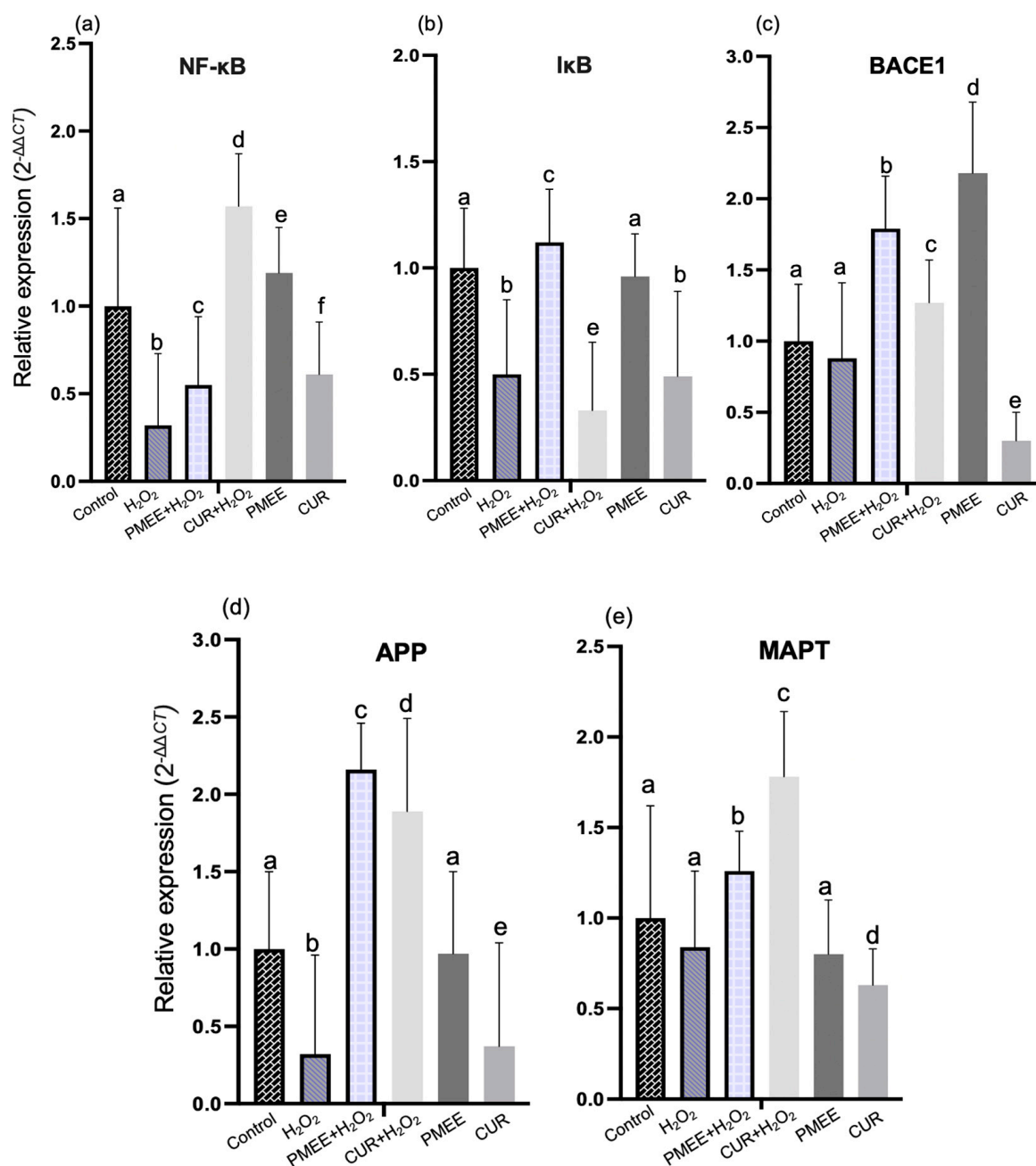


Figure 7. The mRNA expression of (a) NF-κB, (b) IκB, (c) BACE1, (d) APP and (e) MAPT in NF-κB/IκB signaling pathway. Control: untreated cells; H₂O₂: cells induced with 300 μM hydrogen peroxide for 4 h; PMEE+H₂O₂: cells pre-treated with PMEE for 48 h + 4 h exposure to H₂O₂; CUR+H₂O₂: cells pre-treated with curcumin for 48 h + 4 h exposure to H₂O₂; PMEE: cells treated with only PMEE; CUR: cells treated with only curcumin. The value represents fold changes between control (untreated cells) and treatment groups. Data were expressed as the mean ± SD of triplicate experiments; means with different letters denote significant differences with one another and vice versa ($p < 0.05$).

The expression level of the BACE1 gene decreased significantly ($p < 0.05$) in PMEE-treated cells prior to 4 h of H₂O₂ exposure when compared to the expression in H₂O₂ control cells (Figure 7c). In Alzheimer's and Down syndrome disease models, inhibiting the activity of or silencing this gene was associated with neuroprotection [42]. Thus, the genotoxic effect of PMEE on the expression of the BACE1 gene demonstrated the compound's potential to inhibit the functional BACE1 protein's activity. In contrast, 48 h of PMEE pre-treatment

increased APP and MAPT gene expression significantly ($p < 0.05$) in H_2O_2 -treated control cells without PMEE pre-treatment (Figure 7d,e).

2.7. PMEE Pre-Treatment Influenced Gene Expressions in the MAPK Pathway

PMEE pre-treatment prior to H_2O_2 exposure led to a significant ($p < 0.05$) increase in the expression of JNK, p38, and PP2A genes in differentiated cells compared to the expression in H_2O_2 control cells and PMEE only group (Figure 8a,b,d). Curcumin (positive control) could not prevent the genotoxic effect of H_2O_2 on the expression level of JNK, unlike PMEE-treated cells. JNK is a gene that codes for c-Jun N-terminal kinases-3 (JNK3), a neuron-specific isoform protein that plays an essential role in the pathophysiology of a variety of neurological disorders. The upregulation of JNK is activated by H_2O_2 -induced cellular stress. In addition, the p38 gene is a member of the mitogen-activated protein kinase (MAPK) family that plays a crucial role in MAPK pathway-mediated apoptosis [43]. Previous research has demonstrated the neuroprotective effects of PP2A against neuronal apoptosis in cases of traumatic brain injury, acute ischemia, and neurodegenerative disease [44–47]. After 4 h of exposure to H_2O_2 , this indicated that PMEE protects neuroblastoma SH-SY5Y cells from oxidative stress by increasing JNK, p38, and PP2A gene expressions. Meanwhile, the expression level of MKP1 and AKT decreased significantly ($p < 0.05$) in the presence of PMEE pre-treatment prior to H_2O_2 exposure compared to PMEE only treatment group (Figure 8c,f). In contrast, the presence of PMEE did not increase the expression of PP5 under oxidative stress conditions in cells treated with PMEE alone (Figure 8e).

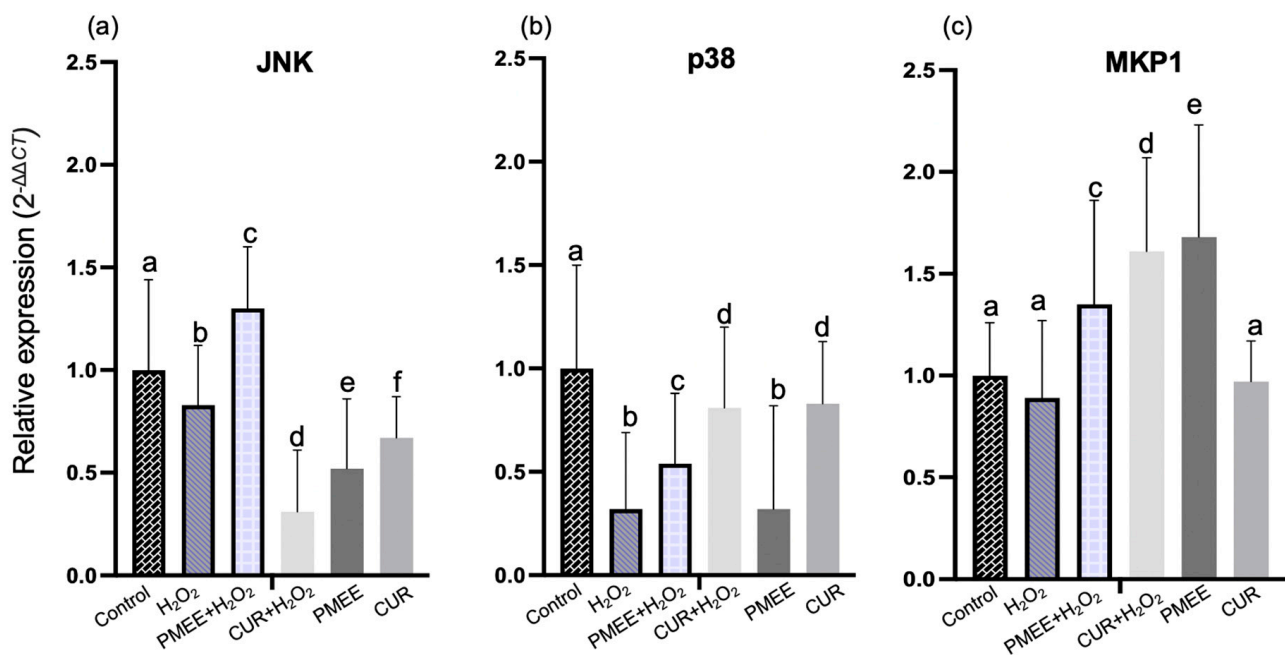


Figure 8. Cont.

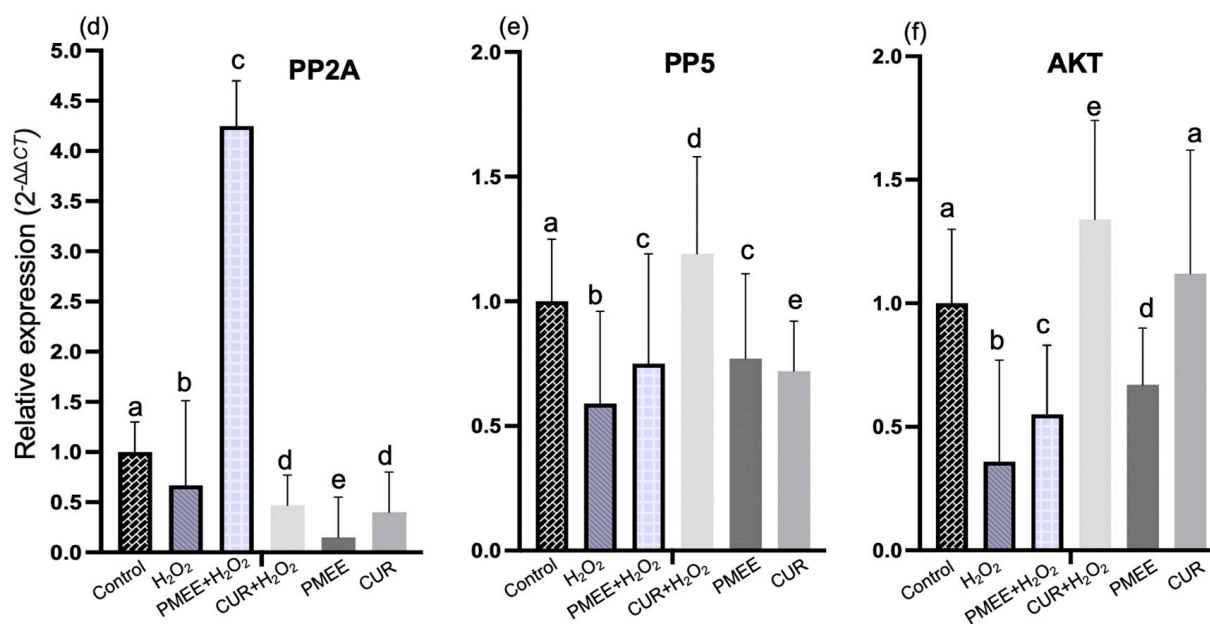


Figure 8. The mRNA expression of (a) JNK, (b) p38, (c) MKP1, (d) PP2A, (e) PP5 and (f) AKT in MAPK signaling pathway. Control: untreated cells; H₂O₂: cells induced with 300 μ M hydrogen peroxide for 4 h; PMEE+H₂O₂: cells pre-treated with PMEE for 48 h + 4 h exposure to H₂O₂; CUR+H₂O₂: cells pre-treated with curcumin for 48 h + 4 h exposure to H₂O₂; PMEE: cells treated with only PMEE; CUR: cells treated with only curcumin. The value represents fold changes between control (untreated cells) and treatment groups. Data were expressed as the mean \pm SD of triplicate experiments; means with different letters denote significant difference ($p < 0.05$).

2.8. PMEE Pre-Treatment Increased the Expression of Acetylcholine (ACH) in SH-SY5Y Differentiated Cells

It has been demonstrated that ACH inhibits the production of ROS during oxidative stress. Therefore, we examined the effects of ACH concentration before or after H₂O₂ treatment on the differentiated SH-SY5Y cells using ELISA. The ACH level in the differentiated SH-SY5Y cells was significantly ($p < 0.05$) increased in PMEE or curcumin pre-treatment prior to 4 h of H₂O₂ exposure compared to that in H₂O₂ control cells as shown in Figure 9. In the present study, PMEE and curcumin have been shown to possess positive effect by increasing the expression of ACH under oxidative conditions.

The potential utilization of herbal medicines as a novel preventative neuroprotective strategy in the context of neurodegenerative illnesses is a subject of interest. These natural therapies could be explored for their applicability in individuals who are at risk of developing such conditions [36]. The AChE is an enzyme that is responsible for the metabolism of the neurotransmitter ACH, and inhibiting AChE can have therapeutic (e.g., Alzheimer's disease drugs) or neurotoxic effects (e.g., pesticides). Patients with coronary artery disease and Alzheimer's disease pathogenesis had elevated ACH gene expression. The finding reported by Işık and Beydemir [48] suggested that an increase in cellular AChE release results in the formation of neurotoxic β -amyloid plaques and may cause neurodegenerative diseases. According to the cholinergic hypothesis, the inhibition of AChE, an enzyme that catalyzes acetylcholine hydrolysis, increases the levels of ACH in the brain, thus improving cholinergic functions in Alzheimer's disease patients. The use of AChE inhibitors has proven to be an effective approach in the management of neurological conditions such as Alzheimer's disease [49]. Therefore, one of the important strategies for treating neurological disease is to maintain the levels of ACH through the inhibition of AChE [50].

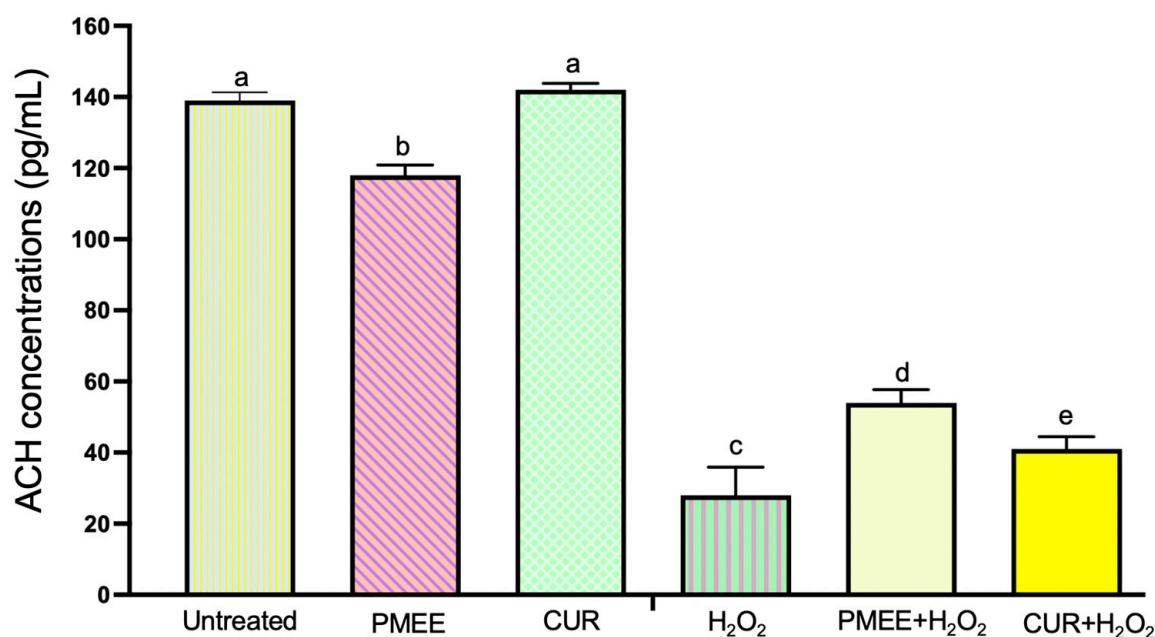


Figure 9. Acetylcholine (ACH) level in the supernatant of differentiated SH-SY5Y cells. The ACH level of cells induced with H₂O₂ increased in both PMEE and CUR-treated cells. Control: untreated cells; H₂O₂: cells induced with 300 μ M hydrogen peroxide for 4 h; PMEE+H₂O₂: cells pre-treated with PMEE for 48 h + 4 h exposure to H₂O₂; CUR+H₂O₂: cells pre-treated with curcumin for 48 h + 4 h exposure to H₂O₂; PMEE: cells treated with only PMEE; CUR: cells treated with only curcumin. The value represents fold changes between control (untreated cells) and treatment groups. Data were expressed as the mean \pm SD of triplicate experiments; means with different letters denote significant differences ($p < 0.05$).

The inhibitory actions of the aqueous and methanolic extracts of *P. minus* leaves were observed on the AChE enzyme [15,51]. A prior research conducted by George et al. [15] demonstrated that the aqueous extract of *P. minus* had inhibitory effects on cholinesterase activity, with an IC₅₀ value of 0.04 mg/mL and a maximal inhibition rate of 68%. The findings of this study indicate that *P. minus* exhibits antioxidant and anticholinesterase properties, and it has been observed to improve cognitive function in vivo and indicates that the extract possesses neuroprotective effects. The AChE inhibitory activity of *P. istanbulicum*, was observed in a dose-dependent manner. The ethanolic extract of *P. istanbulicum* demonstrated the highest level of inhibition against AChE, with an inhibition rate of $88.2 \pm 3.44\%$ as compared to other species of polygonum such as *P. patulum* subsp. *Pulchellum*, *P. aviculare* and *P. lapathifolium* [52]. In this present study, *P. minus* showed promising potential as a therapeutic intervention for Alzheimer's disease due to the observed favorable impact of PMEE on the upregulation of ACH concentrations under oxidative conditions.

2.9. Molecular Docking

The results of molecular docking between PMEE's identified compounds and protein AChE (Protein Data Bank ID: 4EY6) are shown in Table 2. The complexes exhibited comparable binding interaction energy values in the range of -9.5 to -5.8 kcal/mol. The complexes of AChE and quercitrin, aloe-emodin, afzelin and citreorosein showed more negative binding values compared to other compounds, i.e., quercitrin showed the highest docking score at -9.5 kcal/mol followed by aloe-emodin, afzelin, and citreorosein at -9.4 , -9.3 and -9.0 kcal/mol, respectively. Lower binding affinity depicts better ligand receptor interaction as well as higher docking score against AChE.

Table 2. Binding affinity of PMEE's identified compounds with acetylcholinesterase (AChE).

No.	PMEE's Identified Compounds	Binding Affinity to AChE (kcal/mol)
1.	Quercitrin	−9.5
2.	Aloe-emodin	−9.4
3.	Afzelin	−9.3
4.	Citreorosein	−9.0
5.	alpha-Cyperone	−8.7
6.	Quercetin	−8.7
7.	Kaempferol	−8.6
8.	Rhamnetin	−8.6
9.	(2Z)-4,6-dihydroxy-2-[(4-hydroxy-3,5-dimethoxyphenyl)methylidene]-1-benzofuran-3-1	−8.5
10.	6-Hydroxy-3-isopropylidene-4a,5-dimethyl-4,4a,5,6,7,8-hexahydro-2(3H)-naphthalenone	−8.3
11.	Eupatilin	−8.3
12.	Feruloyltyramine	−8.0
13.	Naphtho[2,3-b]furan-9(4H)-1,4,8-bis(acetyloxy)-4a,5,6,7,8a-hexahydro-3,4a,5-trimethyl-, (4S,4aR,5S,8S,8aS)	−7.8
14.	(−)-epicatechin	−7.7
15.	Esculetin	−7.5
16.	Prespatane	−7.5
17.	(2Z)-2-[(E)-6-(hydroxymethyl)-2,4,8,10-tetramethyldodec-2-enylidene]-4-methylpentanedioic acid	−7.3
18.	Daphnetin	−7.3
19.	Valerenic acid	−7.3
20.	Caffeic acids	−7.0
21.	Corynoxene	−7.0
22.	Dibutylphthalate	−7.0
23.	Loliolide	−6.6
24.	5-Hydroxy-2-penten-1-yl-3-oxocyclopentyl acetic acid	−6.5
25.	Carboxymethyl-cyclohexanecarboxylic acid	−6.5
26.	Gallic acid	−6.5
27.	2,3-Dihydroxybenzoic acid	−6.2
28.	Quinic acid	−5.8

Figures 10 and 11 demonstrate results from ligand–protein interaction between AChE and four most active compounds indicated by binding affinity scores (kcal/mol). It showed that the interacting amino acids of AChE and quercitrin were found to be Tyr72, Asp74, Ser 293, and Phe295. Meanwhile, ligand–protein interaction between AChE and the following compounds showed that the interacting amino acids at the active site were found to be Ser293 and Phe295 (aloe-emodin), Tyr72, Asp74, Ser 293, and Gln291 (afzelin), and Tyr72 and Tyr337 (citreorosein). Ligplot analysis showed 2D structure where the hydrogen bonding is in green dashed lines and hydrophobic interaction is in red arcs between AChE with all the different ligands. Furthermore, Pymol analysis showed 3D structure of ligand–protein interactions where the green color indicates the ligand and red color indicates interacting amino acids of the protein.

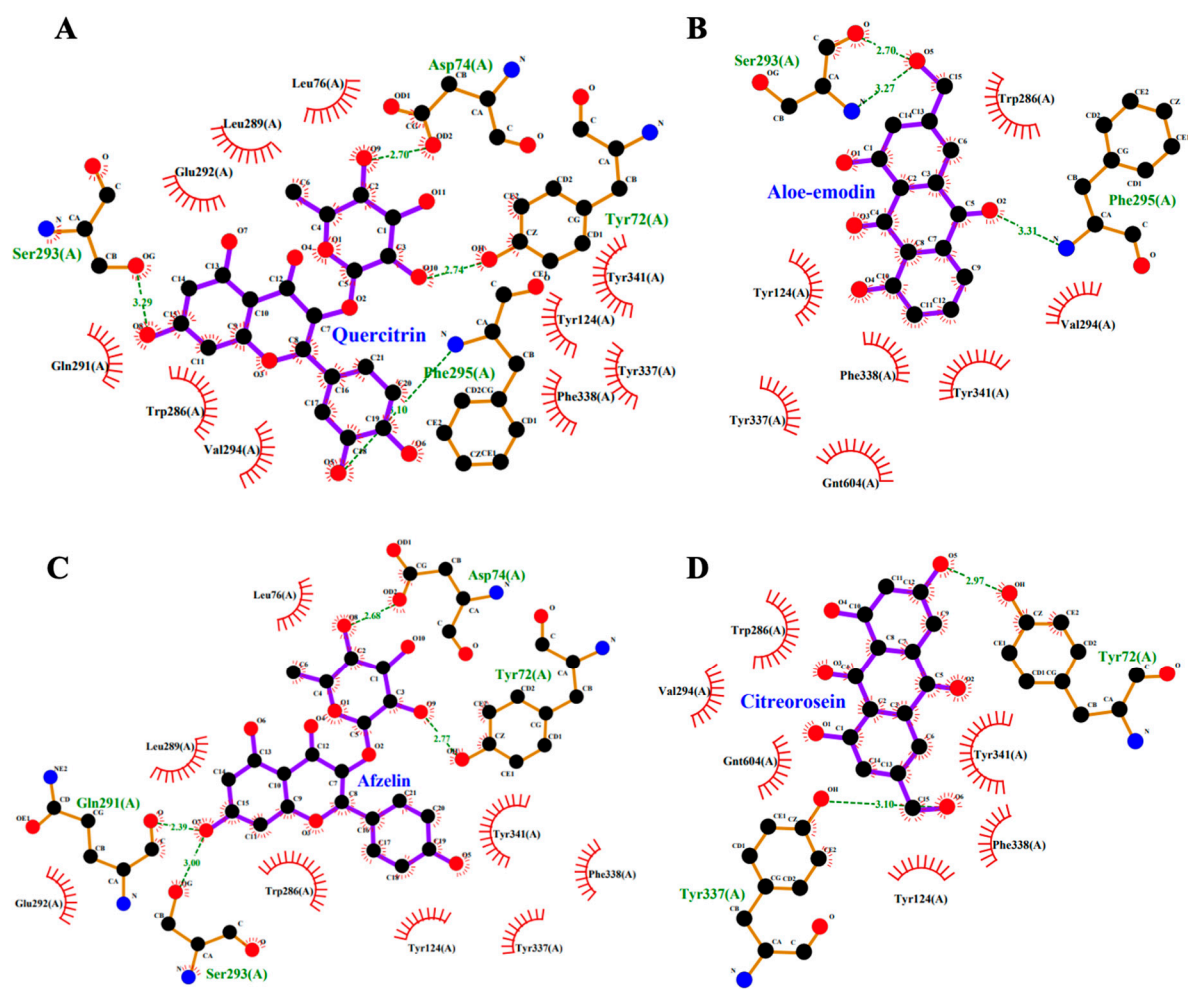


Figure 10. Two-dimensional (2D) interactions of AChE and selected PMEE's identified compounds. (A) Interactions of quercitrin and AChE. (B) Interactions of aloe-emodin and AChE. (C) Interactions of afzelin and AChE. (D) Interactions of citreoresein and AChE.

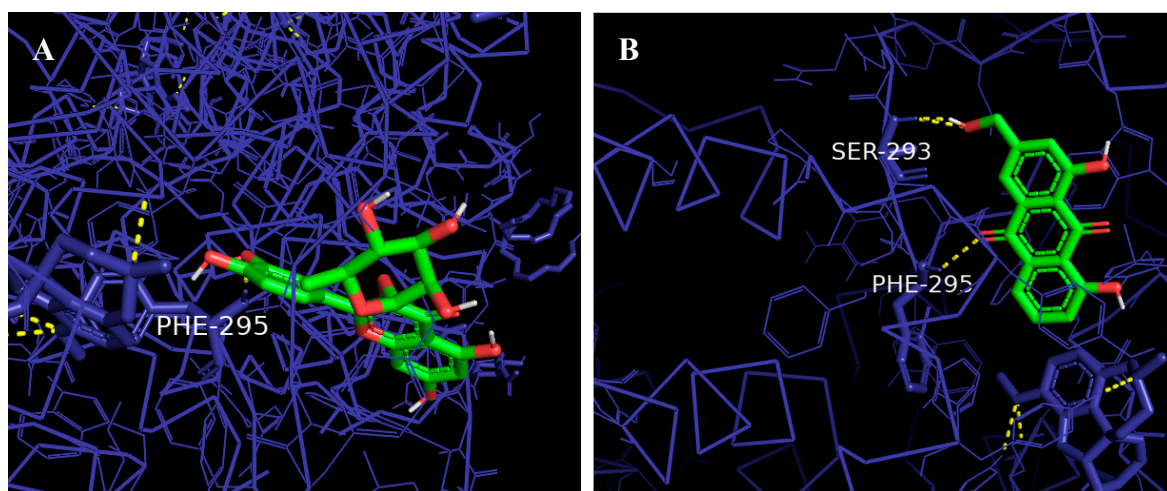


Figure 11. Cont.

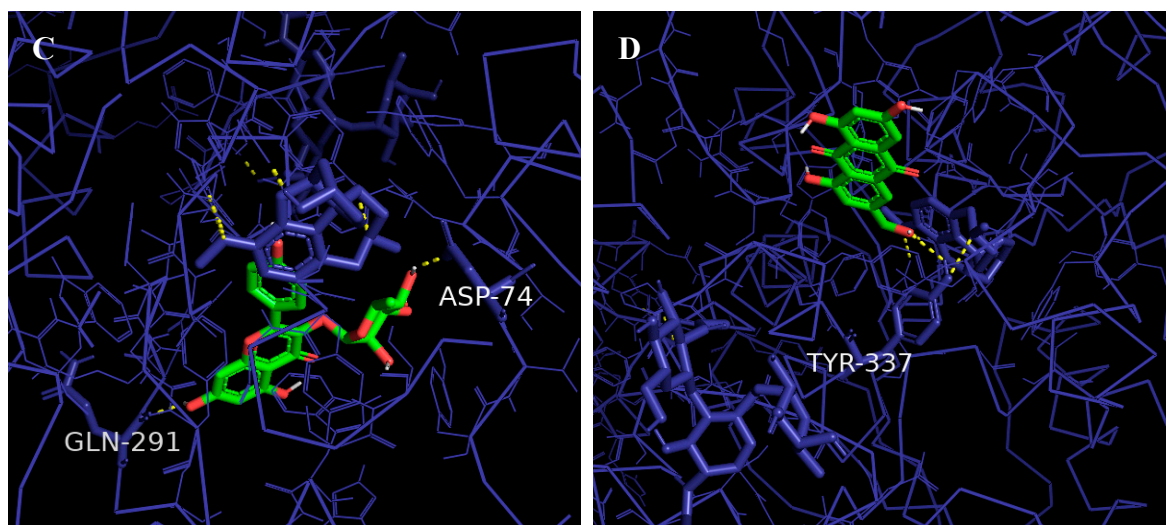


Figure 11. Three-dimensional (3D) interactions of AChE and selected PMEE's identified compounds. Ligands are illustrated in green, AChE protein in dark blue, and hydrogen bonds are depicted in yellow dots. (A) Interactions of quercitrin and AChE. (B) Interactions of aloe-emodin and AChE. (C) Interactions of afzelin and AChE. (D) Interactions of citreoesein and AChE.

3. Materials and Methods

3.1. Plant Collection and Preparation of Ethanolic Extract

P. minus leaves (5 kg) were collected from an experimental plot of INBIOSIS. Original samples (10 kg) were collected from Cameron Highland, Malaysia and a voucher specimen was deposited in the UKMB Herbarium, Universiti Kebangsaan Malaysia. Specimens were identified by a taxonomist and further confirmed by ITS sequencing. *P. minus* leaves (1 kg) were air dried at room temperature (+27 °C) and powdered using a blender (230–250 mesh). Approximately 360 g of leaf powder were soaked in 7.2 L ethanol. The extraction was performed with ratio 1:20 (*w/w*) for 72 h at room temperature. The mixture was filtered, and the filtrate was concentrated using an EYELA OSB-2100 rotary vacuum evaporator model N-11005-WD until complete dryness at 40 °C. Subsequently, the semi-dried ethanol extract was freeze dried using Labconco freeze dryer model 74200-30. The extract was referred to as *P. minus* ethanolic extract (PMEE) and was utilized in subsequent analysis.

3.2. Liquid Chromatography–Mass Spectrometry (LC–MS/MS)

LC–MS/MS was performed with slight modifications to the method described by Bingol and Bursal [53]. The separation was performed using Thermo Scientific (C18 column (Acclaim™ RepMap RSLC, 75 μm × 15 μm, 2 μm, 100 Å) on a Dionex UltiMate 3000 UHPLC system (Thermo Scientific, Waltham, MA, USA). The dry ethanolic extract was dissolved in HPLC-grade methanol. As an internal benchmark, umbelliferon was used. The sample injection volume was 20 μL, and the temperature and flow rate of the column were 60 °C and 0.3 mL/min. The mobile phases were 0.1% formic acid dissolved in water (mobile phase A) and acetonitrile (mobile phase B). The elution was carried out with a 35 min gradient beginning with an increase from 0 to 5% B in the first two minutes, then to 40% B in the next two minutes, and finally to 95% B in the following 16 min. At 95% B, the mixture was held for 2 min prior to an increase of 0.1 min to 100% B. At 100 percent B, the mixture was held for four minutes before dropping to 5 percent B in two minutes. The column (C18, Thermo Scientific) was then reconditioned with the initial gradient for seven minutes. MS/MS analysis was performed using a MicroTOF-QIII (Bruker, Bremen, Germany) system equipped with an electrospray ionization (ESI) source operating in a positive mode of ionization. The nitrogen drying gas was set to 45 psi with a flow rate of 8 L min⁻¹ and a temperature of 200 °C. The voltage of ESI spray was fixed at 4.5 kV, and the voltage of the fragmentor was set at 200 V. For the mass range of 50–1500 *m/z*,

ionization-mode mass spectrum data were recorded. MS-DIAL version 3.70 was utilized for all compound identifications.

3.3. Cell Lines and Cell Cultures

The human neuroblastoma SH-SY5Y cell line was purchased from ATCC, Manassas, VA, USA, (ATCC® CRL-2266™). In this experiment, passage 5 cell lines were used. Dulbecco's Modified Eagle and Hams' 13 media were combined to maintain the cells (DMEM/Hams' F12) (Nacalai, Kyoto, Japan), with 10% fetal bovine serum (FBS), 1% penicillin and streptomycin) and incubated at 37 °C in 5% CO₂ with 95% humidified atmospheric air.

3.4. Neuronal Differentiation of SH-SY5Y Cells

Differentiation of SH-SY5Y cells was achieved in accordance with the stipulated protocol outlined in Jaafaru et al. [31]. According to the predetermined protocol specified by Jaafaru et al. [31] SH-SY5Y cells were successfully differentiated into neuron-like cells. In brief, the cells were seeded in a 6-well plate at a density of 1×10^5 cells/well. Following a 24 h incubation period, each well was added 2 mL of DMEM/F12 media containing 3% heat-inactivated FBS and 10 µM retinoic acid (RA). This was performed in the dark with the incubator set to 37 °C with 5% CO₂. For a period of seven days, the differentiation media was changed every two days. RA-induced differentiation was examined under phase contrast using an inverted light fluorescence microscope (Zeiss Axio Vert A1, Göttingen, Germany) fitted with an image acquisition system (AxioCam MRm, Göttingen, Germany), and multiple images were taken independently.

3.5. Immunocytochemistry (ICC) Assay

To further ascertain the differentiation of SH-SY5Y cells into full neuronal cells by retinoic acid (RA), ICC was conducted according to the protocol described by Jaafaru et al. [31]. The cells were differentiated as previously mentioned after being seeded in 24-well plates at a density of 2×10^4 cells/well. The differentiated cells were washed three times with cold phosphate buffer saline pH 7.4, at 25 °C followed by incubation with 300 µL fixation solution (4% Paraformaldehyde, 1M NaOH and PBS) at 25 °C for 30 min and washed with PBS thereafter. Permeation solution (1% Triton X-100 and 99% PBS) and blocking (0.3% bovine serum albumin, 10% goat serum, 10% tween 20 and PBS) solution were incubated with the cells at 25 °C for 15 min and 30 min, accompanied with washing at each stage. Antibody for class III β-tubulin (Tuj-1), a cytoplasmic neuron-specific protein, was added in ratio of 1:200 blocking solution with subsequent overnight incubation at 4 °C. The cells were washed with PBS the following day and incubated with Alexa fluoropore-488 secondary antibody conjugate (1:200) in the dark at 25 °C for 2 h. Then, the cells were incubated with nuclear counterstaining dye (DAPI dye) for 10 min before images were taken using an inverted light fluorescence microscope (Zeiss Axio Vert A1, Germany) with an image acquisition system (AxioCam MRm, Göttingen, Germany).

3.6. Cytotoxicity of PMEE on the SH-SY5Y Cells

The effect of PMEE on cell viability on differentiated SH-SY5Y cells were assessed using the MTT reduction assay, as modified by Jaafaru et al. [31]. In a 96-well plate, 1×10^4 SH-SY5Y cells were seeded, and they underwent a seven-day period of differentiation process as outlined in Section 3.4. The cells were treated with serially diluted concentrations of PMEE (0.5–1000 µg/mL) for 24, 48, and 72 h to determine how PMEE affected cell viability. The plate was incubated in the dark for four hours after 20 µL addition of MTT solution and then 200 µL of DMSO was added after removal of cell medium to dissolve the formazan that had formed in the wells. Absorbance was measured immediately at 540 nm using a microplate reader. Similar analysis was conducted for H₂O₂ cytotoxic effect, in which 1000 µM concentration was serially diluted to 7.8 µM and the optical density was used to evaluate the IC₅₀ of H₂O₂ used in the present study.

3.7. Neuroprotection of PMEE on the SH-SY5Y Cells

Differentiated SH-SY5Y cells were pre-treated with serial dilutions of PMEE to determine the neuroprotective activity of the PMEE in time-dependent manner prior to 4 h challenged by 220 μM (IC_{50}) H_2O_2 , followed by addition of 20 μL and 200 μL of MTT and DMSO reagent, respectively. Curcumin was used as positive control. The absorbance reading was measured immediately at 540 nm using a microplate reader.

3.8. PMEE Pre-Treatment and H_2O_2 Exposure

The differentiated neuronal cells were seeded in T25 flasks at a density of 1×10^3 cells/mL and underwent differentiation as outlined in Section 3.4. For 48 h, the cells were pre-treated separately with PMEE (6.25 $\mu\text{g}/\text{mL}$) or curcumin (3.13 $\mu\text{g}/\text{mL}$). Prior to bioassay analyses, the pre-treated cells were exposed to 220 μM H_2O_2 for 4 h.

3.9. Gene Expression Study of PMEE-Treated SH-SY5Y Cells

After differentiation and treatment, genomic RNA was extracted using an RNA extraction kit (NucleoSpin RNA Plus, Macherey, Düren, Germany) in accordance with the manufacturer's instructions. The concentration and purity of the isolated RNA were evaluated using Nanodrop spectrophotometer (Thermo Scientific Nanodrop, NanoDrop Technologies, Wilmington, DE, USA). The cDNA was synthesized from one μg of RNA using the HiScript III First Strand cDNA Synthesis kit +gDNA wiper (R312-02, Vazyme, Nanjing, China). Meanwhile, the qPCR was conducted using Maxima SYBR green qPCR Master Mix (Q712-02, Vazyme) according to the manufacturer's instructions. The nucleotide primer sequences used in this study were presented in Table 3. The primers were synthesized by Bio3 Scientific Sdn. Bhd. (Puchong, Malaysia). The glyceraldehyde-3-phosphate dehydrogenase (GAPDH), a housekeeping gene, was used as an internal reference (forward 5'-GTCATCCCTGAGCTGAACGG-3', reverse 5'-AAGTGGTCGTTGAGGGCAAT-3'). Each gene was amplified three times using RT-qPCR. The amplification parameters were as follows: 95 $^\circ\text{C}$ for 30 s, 95 $^\circ\text{C}$ for 5 s, and 60 $^\circ\text{C}$ for 31 s for a total of 40 cycles. Using the $2^{-\Delta\Delta\text{Cq}}$ method, the quantification values were subsequently calculated and analyzed. Ratio in untreated cells (negative control) was assigned as 1.

3.10. Acetylcholine (ACH) Enzyme-Linked Immunosorbent Assay (ELISA)

To detect the ACH release in the culture medium, an ACH enzyme-linked immunosorbent assay (ELISA) (E-EL-0081, Elabscience, Houston, TX, USA) was performed according to the manufacturer's instructions. The cells were cultured in 25 cm^2 flask at a density of 1×10^6 cells/flask and were differentiated as described in Section 3.4. After 7 days, each flask's cell medium was collected and centrifuged for 20 min at $1000 \times g$ and 4 $^\circ\text{C}$. The cell supernatant was collected for the assay. The absorbance value was determined at 550 nm, with the color intensity proportional to the ACH concentration. The concentration of ACH in samples was determined by comparing the absorbance of the samples to the standard curve.

Table 3. Gene name, accession number, forward and reverse primer sequences used in the real-time PCR analysis.

Gene and Accession No	Forward Primer	Reverse Primer
AKT [NM_005465.4]	AGGTGACACTATAGAATA AGACATTAATTTTCCTCGAA	GTACGACTCACTATAGGG AATCCTCATCATATTTTCAGGT
APP [NM_000484.3]	AGGTGACACTATAGAATA CTGTGGCAGACTGAACATGC	GTACGACTCACTATAGGG ATCACCAACTAAGCAGCGGTA
BACE1 [NM_012104.4]	AGGTGACACTATAGAATA CGAGCTGGATTATGGT	GTACGACTCACTATAGGG AGGAGAGGGAGCTTGG

Table 3. Cont.

Gene and Accession No	Forward Primer	Reverse Primer
Catalase [NM_001752.3]	AGGTGACACTATAGAATA AGAAATCCTCAGACACATCT	GTACGACTCACTATAGGG AATGTCATGACCTGGATGTAA
GCLC [NM_001498.3]	AGGTGACACTATAGAATA ATGAAGCAATAAAACAAGCAC	GTACGACTCACTATAGGG ATGGAATGTCACCTGGAG
GST [NM_015917.2]	AGGTGACACTATAGAATA ATACATGGCAAATGACTTAAA	GTACGACTCACTATAGGG ATGATGTCTTCATTCCCTTGAC
HO-1 [NM_002133.2]	AGGTGACACTATAGAATA ACTGCGTTCCTGCTCAACAT	GTACGACTCACTATAGGG AGGGCAGAATCTTGCACTTTGT
IκB [NM_020529.2]	AGGTGACACTATAGAATA CTGCAGCAGACTCCAC	GTACGACTCACTATAGGG AGGGTATTTCTCGAAAGT
JNK [NM_001323327.1]	AGGTGACACTATAGAATA AAGGAAAACGTGGATTTATG	GTACGACTCACTATAGGG ACCAGCATATTTAGGTCTGTT
MAPT [NM_001123066.3]	AGGTGACACTATAGAATA CCCAGATCTGAGAGAGGT	GTACGACTCACTATAGGG ACTTATTAATTATCTGCACCTTCC
MKP1 [NM_004417.3]	AGGTGACACTATAGAATA AGAAGAACCAAATACCTCAA	GTACGACTCACTATAGGG ACAGGTCATAAATAATCAGCA
NF-κB [NM_002908.3]	AGGTGACACTATAGAATA CGTTTTAGATACAAATGTGAAG	GTACGACTCACTATAGGG ACACTTTTCTTTTCCATAAT
NQO1 [NM_000903.2]	AGGTGACACTATAGAATA CTGCGAACTTTCAGTATCC	GTACGACTCACTATAGGG AGAAGGGTCTTTGTCATAC
Nrf2 [NM_006164.4]	AGGTGACACTATAGAATA TCGCAAACAACCTTTTATCT	GTACGACTCACTATAGGG AAGAGGAGGTCTCCGTTA
p38 [NM_001315.2]	AGGTGACACTATAGAATA TGAGCTGAAGATTCTGGA	GTACGACTCACTATAGGG ATGTCAGACGCATAATCTG
PP5 [NM_006247.3]	AGGTGACACTATAGAATA CAAGGACTACGAGAACGCCA	GTACGACTCACTATAGGGA GCTTCACCTTGACCACCGTC
PP2A [NM_002715.3]	AGGTGACACTATAGAATA CCGCCATTACAGAGAG	GTACGACTCACTATAGGGA AGGATTTCTTTAGCCTTCT
SOD1 [NM_000454.4]	AGGTGACACTATAGAATA AAGTACAAAGACAGGAAACG	GTACGACTCACTATAGGGA TGACAAGTTTAATACCCATCT
SOD2 [NM_000636.3]	AGGTGACACTATAGAATA ACAACAGGCCTTATTCC	GTACGACTCACTATAGGGA AGAGCTTAACATACTCAGCA

AKT: serine/threonine protein kinase; APP: amyloid precursor protein; BACE1: β-site amyloid precursor protein cleaving enzyme; GCLC: glutamate-cysteine ligase catalytic; GST: glutathione S transferase; HO-1: heme oxygenase-1; IκB: inhibitory kappa B protein; JNK: C-Jun N-terminal kinase; MAPT: microtubule-associated protein tau; MKP1: mitogen-activated protein kinase phosphatase 1; NF-κB: nuclear factor kappa B; NQO1: NADP quinone oxidoreductase 1; Nrf2: nuclear factor erythroid 2-related factor 2; p38: 38 subunit protein; PP5: protein phosphatase 5; PP2A: serine/threonine protein phosphatase 2A; SOD1: superoxide dismutase 1; SOD2: superoxide dismutase 2.

3.11. Molecular Docking

Molecular docking study was conducted to test the binding affinity of PMEE's identified compounds to AChE enzyme residues. AChE (PDB ID: 4EY6) was retrieved as a PDB file from the RCSB Protein Data Bank (<http://www.rcsb.org/pdb/>, accessed on 15 August 2023). The Auto Dock Tools (version 1.5.7) was used to prepare protein. Crystallographic waters were removed, polar hydrogens were added to a macromolecule, along with Kollman charges. To get the best conformational docking state, a grid box covering the active site residues of the target protein was created. Using AutoDock Tools 1.5.7, the docking search site was established where ligands could investigate potential binding interactions with AChE [54]. The 3D cuboidal AutoGrid box's center was set to (x: 12.3199, y: 42.071, z: 28.832), and its dimensions were set to (x: 24 y: 20 z: 20) for the number of points.

The molecular docking runs were carried out using command prompt. The AutoDock Vina software, target receptor and ligand pdbqt files, configuration text file, and intended destination of output data were all supplied in the docking command line. The resulting AutoDock Vina output files in pdbqt format contained the generated poses as well as text data listing the relevant poses' binding energies [55]. The binding affinity measured in terms of binding energy (kcal/mol) and the visualization of binding conformation for each docking mode using PyMOL were the two results from molecular docking.

3.12. Statistical Analysis

Data are presented as the mean standard deviation, and differences between means of each group were determined by one-way analysis of variance (ANOVA) with Tukey's multiple comparison, using Graph Pad Prism 9 (GraphPad Software, Inc., San Diego, CA, USA). The 95% confidence interval was considered, thus $p < 0.05$ signified statistical significance.

4. Conclusions

This study revealed the ability of PMEE to halt ROS generation due to oxidative stress induced by H_2O_2 . The findings showed that the demonstrated effects were coordinated through the Nrf2/ARE, NF- κ B/I κ B, and MAPK signaling pathways, thus concluding that PMEE confers neuroprotection against oxidative stress in differentiated SH-SY5Y cells. Quercitrin had the best docking score compared to the other compounds found in PMEE, which had lower docking scores. The present study suggests that PMEE may be a potential therapeutic agent for the treatment of neurodegenerative disorders associated with oxidative stress. The results of our study provide a justification for further investigation into the application of PMEE in animal models of neurodegenerative disorders, in order to assess their safety and effectiveness. Additionally, this would serve as a fundamental basis for subsequent clinical investigations.

Author Contributions: Conceptualization, N.H.S., S.N.B., N.S. and M.N.S.; methodology, N.H.S., M.N.S., N.Z. and J.K.T.; software, N.H.S., N.Z., Q.U.A. and J.K.T.; validation, N.H.S., M.N.S., H.S.H., H.B. and N.S.; formal analysis, N.H.S., Q.U.A. and M.N.S.; investigation: N.H.S.; resources, M.N.S.; writing—original draft preparation, N.H.S.; writing—review and editing, N.H.S., M.N.S., H.S.H., H.B., Q.U.A., H.P., S.M., M.A.A. and N.S.; supervision, M.N.S., N.S. and J.K.T.; funding acquisition, M.N.S., H.P., S.M. and M.A.A. All authors have read and agreed to the published version of the manuscript.

Funding: The present study was supported by Geran Galakan Penyelidik Muda, Universiti Kebangsaan Malaysia (GGPM-2020-037).

Institutional Review Board Statement: Not applicable.

Informed Consent Statement: Not applicable.

Data Availability Statement: Not applicable.

Acknowledgments: The authors wish to thank UPM-MAKNA Cancer Research Laboratory, Institute of Bioscience, Universiti Putra Malaysia for support and facilities.

Conflicts of Interest: The authors declare no conflict of interest.

Sample Availability: Not applicable.

References

1. Singh, A.; Kukreti, R.; Saso, L.; Kukreti, S. Oxidative Stress: A Key Modulator in Neurodegenerative Diseases. *Molecules* **2019**, *24*, 1583. [[CrossRef](#)] [[PubMed](#)]
2. Liguori, I.; Russo, G.; Curcio, F.; Bulli, G.; Aran, L.; Della-Morte, D.; Gargiulo, G.; Testa, G.; Cacciatore, F.; Bonaduce, D.; et al. Oxidative stress, aging, and diseases. *Clin. Interv. Aging* **2018**, *13*, 757. [[CrossRef](#)] [[PubMed](#)]
3. Sharifi-Rad, M.; Anil Kumar, N.V.; Zucca, P.; Varoni, E.M.; Dini, L.; Panzarini, E.; Rajkovic, J.; Tsouh Fokou, P.V.; Azzini, E.; Peluso, I.; et al. Lifestyle, Oxidative Stress, and Antioxidants: Back and Forth in the Pathophysiology of Chronic Diseases. *Front. Physiol.* **2020**, *11*, 694. [[CrossRef](#)] [[PubMed](#)]

4. Lobo, V.; Patil, A.; Phatak, A.; Chandra, N. Free radicals, antioxidants and functional foods: Impact on human health. *Pharmacogn. Rev.* **2010**, *4*, 118–126. [[CrossRef](#)]
5. Kurutas, E.B. The importance of antioxidants which play the role in cellular response against oxidative/nitrosative stress: Current state. *Nutr. J.* **2016**, *15*, 71. [[CrossRef](#)]
6. Ahmad, R.; Rosandy, A.R.; Sahidin, I.; Ab Ghani, N.S.; Noor, N.M.; Baharum, S.N. Bioassay Analysis and Molecular Docking Study Revealed the Potential Medicinal Activities of Active Compounds Polygonumins B, C and D from *Polygonum minus* (*Persicaria minor*). *Plants* **2023**, *12*, 59. [[CrossRef](#)]
7. Seimandi, G.; Álvarez, N.; Stegmayer, M.I.; Fernández, L.; Ruiz, V.; Favaro, M.A.; Derita, M. An Update on Phytochemicals and Pharmacological Activities of the Genus *Persicaria* and *Polygonum*. *Molecules* **2021**, *26*, 5956. [[CrossRef](#)]
8. Vikram, P.; Chiruvella, K.K.; Ripain, I.H.A.; Arifullah, M. A recent review on phytochemical constituents and medicinal properties of kesum (*Polygonum minus* Huds.). *Asian Pac. J. Trop. Biomed.* **2014**, *4*, 430–435. [[CrossRef](#)]
9. Hamid, A.A.; Aminuddin, A.; Yunus, M.H.M.; Murthy, J.K.; Hui, C.K.; Ugusman, A. Antioxidative and anti-inflammatory activities of *Polygonum minus*: A review of literature. *Rev. Cardiovasc. Med.* **2020**, *21*, 275–288. [[CrossRef](#)]
10. Maizura, M.; Abdullah, A.; Mustapha, W. Total phenolic content and antioxidant activity of kesum (*Polygonum minus*), ginger (*Zingiber officinale*) and turmeric (*Curcuma longa*) extract. *Int. Food Res. J.* **2011**, *18*, 526–531.
11. Nadzirah, A.S.; Rusop, M.; Noriham, A. A review of potential of antioxidant properties using *Polygonum minus*. *Adv. Mater. Res.* **2014**, *832*, 659–664. [[CrossRef](#)]
12. Abdullah, M.Z.; Mohd Ali, J.; Abolmaesoomi, M.; Abdul-Rahman, P.S.; Hashim, O.H. Anti-proliferative, in vitro antioxidant, and cellular antioxidant activities of the leaf extracts from *Polygonum minus* Huds: Effects of solvent polarity. *Int. J. Food Prop.* **2017**, *20*, 846–862. [[CrossRef](#)]
13. Wasman, S.Q.; Mahmood, A.A.; Salehuddin, H.; Zahra, A.A.; Salmah, I. Cytoprotective activities of *Polygonum minus* aqueous leaf extract on ethanol-induced gastric ulcer in rats. *J. Med. Plants Res.* **2010**, *4*, 2658–2665. [[CrossRef](#)]
14. Christopher, P.; Parasuraman, S.; Christina, J.; Asmawi, M.Z.; Vikneswaran, M. Review on *Polygonum minus*. Huds, a commonly used food additive in Southeast Asia. *Pharmacogn. Res.* **2015**, *7*, 1–6. [[CrossRef](#)] [[PubMed](#)]
15. George, A.; Ng, C.P.; O’Callaghan, M.; Jensen, G.S.; Wong, H.J. In vitro and ex-vivo cellular antioxidant protection and cognitive enhancing effects of an extract of *Polygonum minus* Huds (LineminusTM) demonstrated in a Barnes Maze animal model for memory and learning. *BMC Complement. Altern. Med.* **2014**, *14*, 161. [[CrossRef](#)]
16. Almey, A.; Khan, A.J.; Zahir, S.; Suleiman, M.; Aisyah, M.R.; Rahim, K. Total phenolic content and primary antioxidant activity of methanolic and ethanolic extracts of aromatic plants’ leaves. *Int. Food Res. J.* **2010**, *17*, 1077–1084.
17. Faujan, H.; Noriham, A.; Norrakiah, B. Antioxidative Activities of Water Extracts of Some Malaysian Herbs 61. *ASEAN Food J.* **2007**, *14*, 61–68.
18. Kähkönen, M.P.; Hopia, A.I.; Vuorela, H.J.; Rauha, J.-P.; Pihlaja, K.; Kujala, T.S.; Heinonen, M. Antioxidant Activity of Plant Extracts Containing Phenolic Compounds. *J. Agric. Food Chem.* **1999**, *47*, 3954–3962. [[CrossRef](#)]
19. Ahmad, R.; Sahidin, I.; Taher, M.; Low, C.; Noor, N.M.; Sillapachaiyaporn, C.; Chuchawankul, S.; Sarachana, T.; Tencomnao, T.; Iskandar, F.; et al. Polygonumins A, a newly isolated compound from the stem of *Polygonum minus* Huds with potential medicinal activities. *Sci. Rep.* **2018**, *8*, 4202. [[CrossRef](#)]
20. Yaacob, K.B. Kesom Oil-A Natural Source of Aliphatic Aldehydes. *Perfum. Flavor.* **1987**, *12*, 28–30.
21. Baharum, S.N.; Bunawan, H.; Ghani, M.A.; Wan Mustapha, W.A.; Noor, N.M. Analysis of the Chemical Composition of the Essential Oil of *Polygonum minus* Huds. Using Two-Dimensional Gas Chromatography-Time-of-Flight Mass Spectrometry (GC-TOF MS). *Molecules* **2010**, *15*, 7006. [[CrossRef](#)] [[PubMed](#)]
22. Ruijters, E.J.B.; Weseler, A.R.; Kicken, C.; Haenen, G.R.M.M.; Bast, A. The flavanol (-)-epicatechin and its metabolites protect against oxidative stress in primary endothelial cells via a direct antioxidant effect. *Eur. J. Pharmacol.* **2013**, *715*, 147–153. [[CrossRef](#)] [[PubMed](#)]
23. Du, L.; Chen, J.; Xing, Y. Eupatilin prevents H₂O₂-induced oxidative stress and apoptosis in human retinal pigment epithelial cells. *Biomed. Pharmacother.* **2017**, *85*, 136–140. [[CrossRef](#)] [[PubMed](#)]
24. Yang, C.; Yang, W.; He, Z.; Guo, J.; Yang, X.; Wang, R.; Li, H. Kaempferol Alleviates Oxidative Stress and Apoptosis Through Mitochondria-dependent Pathway During Lung Ischemia-Reperfusion Injury. *Front. Pharmacol.* **2021**, *12*, 624402. [[CrossRef](#)]
25. Shojaee, M.S.; Moeenfar, M.; Farhoosh, R. Kinetics and stoichiometry of gallic acid and methyl gallate in scavenging DPPH radical as affected by the reaction solvent. *Sci. Rep.* **2022**, *12*, 8765. [[CrossRef](#)]
26. Khan, F.A.; Maalik, A.; Murtaza, G. Inhibitory mechanism against oxidative stress of caffeic acid. *J. Food Drug Anal.* **2016**, *24*, 695–702. [[CrossRef](#)]
27. Medeiros, D.L.; Lima, E.T.G.; Silva, J.C.; Medeiros, M.A.; Pinheiro, E.B.F. Rhamnetin: A review of its pharmacology and toxicity. *J. Pharm. Pharmacol.* **2022**, *74*, 793–799. [[CrossRef](#)]
28. Dai, X.; Ding, Y.; Zhang, Z.; Cai, X.; Li, Y. Quercetin and quercitrin protect against cytokine-induced injuries in RINm5F β -cells via the mitochondrial pathway and NF- κ B signaling. *Int. J. Mol. Med.* **2013**, *31*, 265–271. [[CrossRef](#)]
29. Kwon, Y.K.; Choi, S.J.; Kim, C.R.; Kim, J.K.; Kim, Y.-J.; Choi, J.H.; Song, S.-W.; Kim, C.-J.; Park, G.G.; Park, C.-S.; et al. Antioxidant and cognitive-enhancing activities of *Arctium lappa* L. roots in A β 1-42-induced mouse model. *Appl. Biol. Chem.* **2016**, *59*, 553–565. [[CrossRef](#)]

30. Cimini, A.; Ardini, M.; Gentile, R.; Giansanti, F.; Benedetti, E.; Cristiano, L.; Fidoamore, A.; Scotti, S.; Panella, G.; Angelucci, F.; et al. A peroxiredoxin-based proteinaceous scaffold for the growth and differentiation of neuronal cells and tumour stem cells in the absence of prodifferentiation agents. *J. Tissue Eng. Regen. Med.* **2016**, *11*, 2462–2470. [[CrossRef](#)]
31. Jaafaru, M.S.; Nordin, N.; Shaari, K.; Rosli, R.; Abdull Razis, A.F. Isothiocyanate from *Moringa oleifera* seeds mitigates hydrogen peroxide-induced cytotoxicity and preserved morphological features of human neuronal cells. *PLoS ONE* **2018**, *13*, e0196403. [[CrossRef](#)] [[PubMed](#)]
32. Ismail, N.; Ismail, M.; Imam, M.U.; Azmi, N.H.; Fathy, S.F.; Foo, J.B.; Abu Bakar, M.F. Mechanistic basis for protection of differentiated SH-SY5Y cells by oryzanol-rich fraction against hydrogen peroxide-induced neurotoxicity. *BMC Complement. Altern. Med.* **2014**, *14*, 467. [[CrossRef](#)] [[PubMed](#)]
33. Qader, S.W.; Abdulla, M.A.; Chua, L.S.; Najim, N.; Zain, M.M.; Hamdan, S. Antioxidant, total phenolic content and cytotoxicity evaluation of selected Malaysian plants. *Molecules* **2011**, *16*, 3433–3443. [[CrossRef](#)]
34. Mohd Ghazali, M.A.; Al-Naqeb, G.; Krishnan Selvarajan, K.; Hazizul Hasan, M.; Adam, A. Apoptosis Induction by *Polygonum minus* is Related to Antioxidant Capacity, Alterations in Expression of Apoptotic-Related Genes, and S-Phase Cell Cycle Arrest in HepG2 Cell Line. *Biomed. Res. Int.* **2014**, *2014*, 539607. [[CrossRef](#)]
35. Zhao, X.; Fang, J.; Li, S.; Gaur, U.; Xing, X.; Wang, H.; Zheng, W. Artemisinin Attenuated Hydrogen Peroxide (H₂O₂)-Induced Oxidative Injury in SH-SY5Y and Hippocampal Neurons via the Activation of AMPK Pathway. *Int. J. Mol. Sci.* **2019**, *20*, 2680. [[CrossRef](#)]
36. Shen, B.; Truong, J.; Helliwell, R.; Govindaraghavan, S.; Sucher, N.J. An in Vitro Study of Neuroprotective Properties of Traditional Chinese Herbal Medicines Thought to Promote Healthy Ageing and Longevity. *BMC Complement. Altern. Med.* **2013**, *13*, 373. [[CrossRef](#)] [[PubMed](#)]
37. Lee, D.Y.; Song, M.Y.; Kim, E.H. Role of Oxidative Stress and Nrf2/KEAP1 Signaling in Colorectal Cancer: Mechanisms and Therapeutic Perspectives with Phytochemicals. *Antioxidants* **2021**, *10*, 743. [[CrossRef](#)] [[PubMed](#)]
38. Singh, R.R.; Reindl, K.M. Glutathione S-Transferases in Cancer. *Antioxidants* **2021**, *10*, 701. [[CrossRef](#)] [[PubMed](#)]
39. Wang, Y.; Branicky, R.; Noë, A.; Hekimi, S. Superoxide dismutases: Dual roles in controlling ROS damage and regulating ROS signaling. *J. Cell Biol.* **2018**, *217*, 1915. [[CrossRef](#)] [[PubMed](#)]
40. Nandi, A.; Yan, L.J.; Jana, C.K.; Das, N. Role of Catalase in Oxidative Stress- and Age-Associated Degenerative Diseases. *Oxidative Med. Cell. Longev.* **2019**, *2019*, 9613090. [[CrossRef](#)] [[PubMed](#)]
41. Nijboer, C.H.A.; Heijnen, C.J.; Groenendaal, F.; May, M.J.; Van Bel, F.; Kavelaars, A. Strong Neuroprotection by Inhibition of NF- κ B after Neonatal Hypoxia-Ischemia Involves Apoptotic Mechanisms but is Independent of Cytokines. *Stroke* **2008**, *39*, 2129–2137. [[CrossRef](#)]
42. Chen, C.H.; Zhou, W.; Liu, S.; Deng, Y.; Cai, F.; Tone, M.; Tone, Y.; Tong, Y.; Song, W. Increased NF- κ B signalling up-regulates BACE1 expression and its therapeutic potential in Alzheimer's disease. *Int. J. Neuropsychopharmacol.* **2012**, *15*, 77–90. [[CrossRef](#)] [[PubMed](#)]
43. Miller, A.L.; Webb, M.S.; Copik, A.J.; Wang, Y.; Johnson, B.H.; Kumar, R.; Thompson, E.B. p38 Mitogen-Activated Protein Kinase (MAPK) Is a Key Mediator in Glucocorticoid-Induced Apoptosis of Lymphoid Cells: Correlation between p38 MAPK Activation and Site-Specific Phosphorylation of the Human Glucocorticoid Receptor at Serine 211. *Mol. Endocrinol.* **2005**, *19*, 1569–1583. [[CrossRef](#)] [[PubMed](#)]
44. Cipriani, R.; Chara, J.C.; Rodríguez-Antigüedad, A.; Matute, C. FTY720 attenuates excitotoxicity and neuroinflammation. *J. Neuroinflamm.* **2015**, *12*, 86. [[CrossRef](#)] [[PubMed](#)]
45. Majd, S.; Power, J.H.T.; Koblar, S.A.; Grantham, H.J.M. Early glycogen synthase kinase-3 β and protein phosphatase 2A independent tau dephosphorylation during global brain ischaemia and reperfusion following cardiac arrest and the role of the adenosine monophosphate kinase pathway. *Eur. J. Neurosci.* **2016**, *44*, 1987–1997. [[CrossRef](#)]
46. Sangodkar, J.; Farrington, C.C.; McClinch, K.; Galsky, M.D.; Kastrinsky, D.B.; Narla, G. All roads lead to PP2A: Exploiting the therapeutic potential of this phosphatase. *FEBS J.* **2016**, *283*, 1004–1024. [[CrossRef](#)]
47. Tan, X.L.; Wright, D.K.; Liu, S.; Hovens, C.; O'Brien, T.J.; Shultz, S.R. Sodium selenate, a protein phosphatase 2A activator, mitigates hyperphosphorylated tau and improves repeated mild traumatic brain injury outcomes. *Neuropharmacology* **2016**, *108*, 382–393. [[CrossRef](#)]
48. Işık, M.; Beydemir, Ş. AChE mRNA expression as a possible novel biomarker for the diagnosis of coronary artery disease and Alzheimer's disease, and its association with oxidative stress. *Arch. Physiol. Biochem.* **2019**, *128*, 352–359. [[CrossRef](#)]
49. Attar, U.A.; Ghane, S.G. In Vitro Antioxidant, Antidiabetic, Antiacetylcholine Esterase, Anticancer Activities and RP-HPLC Analysis of Phenolics from the Wild Bottle Gourd (*Lagenaria siceraria* (Molina) Standl.). *S. Afr. J. Bot.* **2019**, *125*, 360–370. [[CrossRef](#)]
50. Khan, H.; Maryal, Amin, S.; Kamal, M.A.; Patel, S. Flavonoids as acetylcholinesterase inhibitors: Current therapeutic standing and future prospects. *Biomed. Pharmacother.* **2018**, *101*, 860–870. [[CrossRef](#)]
51. Ahmad, R.; Baharum, S.; Bunawan, H.; Lee, M.; Mohd Noor, N.; Rohani, E.R.; Ilias, N.; Zin, N.M. Volatile profiling of aromatic traditional medicinal plant, *Polygonum minus* in different tissues and its biological activities. *Molecules* **2014**, *19*, 19220–19242. [[CrossRef](#)] [[PubMed](#)]
52. Yilmaz-Ozden, T.; Nasabi, N.T.; Hasbal-Celikok, G.; Kocyigit, M.; Özhan, G. Antioxidant, Anti-Acetylcholinesterase, and Anticancer Activities of Four *Polygonum* Species from Istanbul. *Int. Food Res. J.* **2021**, *28*, 1298–1309. [[CrossRef](#)]

53. Bingol, M.N.; Bursal, E. LC-MS/MS Analysis of Phenolic Compounds and In Vitro Antioxidant Potential of *Stachys lavandulifolia* Vahl. var. *brachydon* Boiss. *Int. Lett. Nat. Sci.* **2018**, *72*, 28–36. [[CrossRef](#)]
54. Morris, G.M.; Ruth, H.; Lindstrom, W.; Sanner, M.F.; Belew, R.K.; Goodsell, D.S.; Olson, A.J. Software news and updates AutoDock4 and AutoDockTools4: Automated docking with selective receptor flexibility. *J. Comput. Chem.* **2009**, *30*, 2785–2791. [[CrossRef](#)]
55. Trott, O.; Olson, A.J. AutoDock Vina: Improving the speed and accuracy of docking with a new scoring function, efficient optimization, and multithreading. *J. Comput. Chem.* **2010**, *31*, 455–461. [[CrossRef](#)]

Disclaimer/Publisher’s Note: The statements, opinions and data contained in all publications are solely those of the individual author(s) and contributor(s) and not of MDPI and/or the editor(s). MDPI and/or the editor(s) disclaim responsibility for any injury to people or property resulting from any ideas, methods, instructions or products referred to in the content.